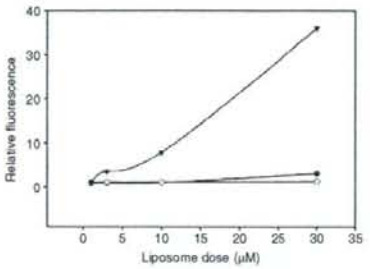

Figure 5 Total cell-associated fluorescence of human umbilical vein endothelial cell (HUVEC) after incubation with CXCR4-targeted liposomes and control liposomes. After the HUVECs attached themselves to the plate, the medium was replaced with media with or without 100 ng/ml vascular endothelial growth factor-A (VEGF-A). After 16 hours the cells were incubated for 1 hour with fluorescently labeled liposomes, and the total cell-associated fluorescence was measured. Closed circles, untargeted liposomes; open circles, CXCR4-targeted liposomes no VEGF stimulation; closed inverted triangles, CXCR4-targeted liposomes after 16 hours of stimulation of HUVECs with 100 ng/ml VEGF-A.

same extent as untargeted control liposomes. However, when the cells were incubated overnight with 100 ng/ml recombinant rat VEGF164, the amount of cell-surface-associated CXCR4-targeted liposomes increased in a dose-dependent manner. At the highest dose of 30 μmol/l lipid, CXCR4-targeted liposomes were shown to bind ninefold more effectively than the untargeted controls (**Figure 5**).

The combined results of fluorescence-activated cell sorting and liposome-uptake measurements showed that the increase in receptor-density on HUVECs (induced by VEGF) resulted in increased cell uptake of the liposomes. This effect could not have been caused by increased cell proliferation in response to VEGF-stimulation, because liposomes lacking the peptide did not bind to the cells whether VEGF was present or not (data not shown). In addition, CXCR4-targeted liposomes were not taken up by the cells that lacked VEGF treatment, further demonstrating that uptake is receptor-mediated and not caused by non-specific binding.

VEGF-A induces CXCR4 expression on mesenteric endothelial cells in the blood vessel organ culture

In order to test how targeted lipoplexes interact with endothelial cells in a more biologically relevant context than conventional cell culture, an organ culture of mesenteric rat-arteries was developed. Dissected arteries from the mesentery can be mounted on a custom-made perfusion system and kept viable for up to 4 days. This provides a three-dimensional model-system comprised of an intact mesenteric artery, and it can be monitored continuously using standard microscopy. **Figure 6a** shows a picture of the apparatus; the ends of the dissected mesenteric arteries are slipped over two glass cannulas inserted in a Petri-dish. **Figure 6b** shows the glass cannulas, the mounted artery, and the sutures used. **Figure 6c–e** shows Hoechst (panel c) and propidium iodide (panel d) stains of a vessel that has been in culture for 4 days. The left side of the blood vessel has been handled with forceps in order to mount the artery on the glass cannula, and this explains the

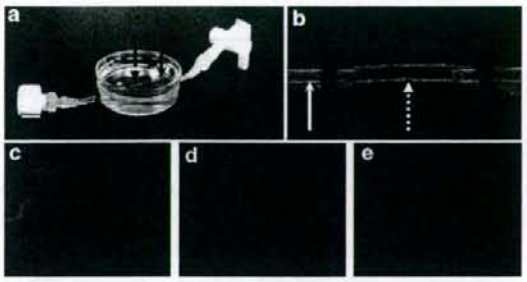

Figure 6 *Ex vivo* artery culture apparatus for mesenteric rat arteries. The blood vessels were mounted on cannulas and maintained at 37 °C for 4 days. (**a**) The custom-made perfusion system. (**b**) A mounted artery observed under a low magnification. The artery (arrow with broken line) is mounted on the glass cannula (arrows). (**c**) Hoechst nuclear stain (blue); smooth muscle cells are seen perpendicular to the plane of the vessel, whereas endothelial cells are parallel to the plane. (**d**) Propidium iodide stain (red) identifies dead cells. (**e**) Merged view of **c** and **d**.

cell-death observed at that end. Throughout the rest of the blood vessel most of the cells remain viable.

In order to confirm that CXCR4 surface expression on endothelial cells of the blood vessel is regulated by VEGF in a fashion similar to that observed for HUVECs, arteries were incubated with 100 ng/ml rrVEGF164 overnight and stained for CXCR4 using indirect immunohistochemistry. The results are shown in **Figure 7a–d**. In the mesenteric artery culture it can be clearly seen that CXCR4 is abundantly expressed on endothelial cells only after incubation with VEGF, as indicated by the green fluorescence (**Figure 7d**). The arteries that were not incubated with VEGF, and the negative controls, only show diffuse green auto-fluorescence caused by the curvature of the organ culture, and this is clearly distinguishable from the punctuated CXCR4-positive cell staining, indicated by arrows (**Figure 7d**).

These pictures show that CXCR4 surface expression is induced by perfusing the blood vessel with VEGF-A. This method provides an opportunity to study the interaction of targeted lipoplexes with endothelial cells of the artery in a biologically very relevant, three-dimensional model system.

CXCR4-targeted lipoplexes bind specifically to mesentric endothelial cells expressing the receptor

In order to assess whether CXCR4-ligand targeted lipoplexes would bind specifically to endothelial cells of mesenteric arteries in the organ culture model, rhodamine-labeled transfection-complexes were formulated with empty vector plasmid (pVC1157). After slowly perfusing the labeled complexes through the blood vessel, incubating for 30 minutes, and washing the artery lumen extensively, red fluorescence was visualized. Again we observed similar results as in the liposome binding study with HUVECs. Arteries (both with and without VEGF-treatment) that had been incubated with untargeted complexes displayed only a very faint background fluorescence (data not shown). Also, vessels that had not been stimulated with rrVEGF164 overnight and incubated with CXCR4-targeted lipoplexes showed only faint diffuse fluorescence (**Figure 7g**). This was in sharp contrast to what was observed in

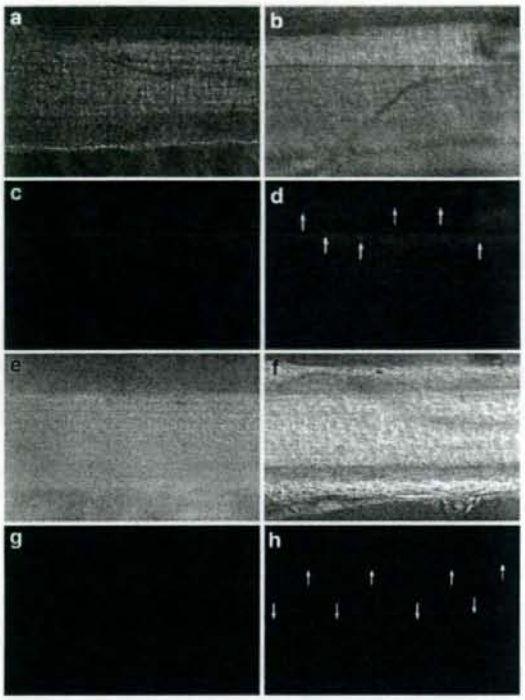

Figure 7 Vascular endothelial growth factor-A induced CXCR4-expression and endothelial cell-specific binding of CXCR 4-targeted lipoplexes in an organ culture of a rat mesenteric blood vessel. (**a-d**) Indirect immunohistochemical staining for CXCR4. (**a**, **b**) Bright field pictures outlining the blood vessel. In **c** and **d**, green represents fluorescent-5-isothiocyanate stained CXCR4-positive endothelial cells. CXCR4-receptor expression is indicated by arrows in **d**. (**e-f**) Perfusion with fluorescent lipoplexes. (**e**, **f**) Bright field images. In **g** and **h**, red represents thodamine-labeled lipoplexes to the endothelial cells. The blood vessels were perfused with (**a**,**c**,**e**, and **g**) saline, or (**b**, **d**, **f**, and **h**) 100 ng/ml rrVEGF164, and incubated at 37°C overnight. At least two independent experiments were performed for each set of conditions. Representative sections are shown. Original magnification: ×200.

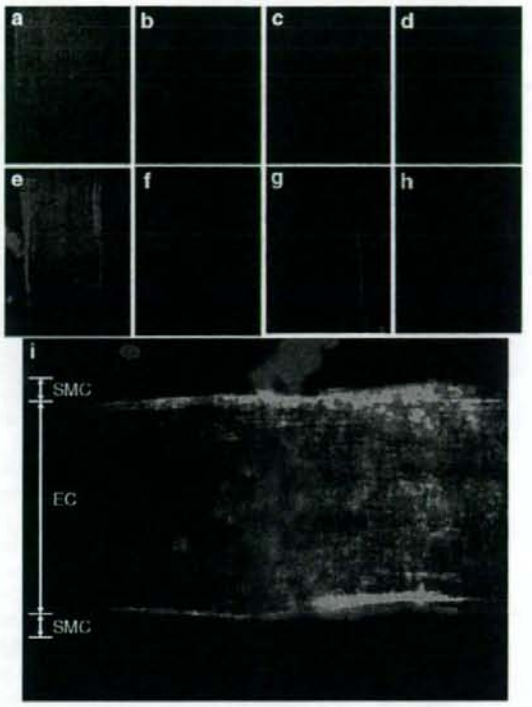

Figure 8 Green fluorescent protein (GFP)-expression in an organ culture of a rat mesenteric blood vessel with CXCR4-targeted lipoplexes. The blood vessels were perfused with (**a–d**) saline or (**e–i**) 100 ng/ml rrVEGF164, and incubated at 37°C overnight before transfection with CXCR4-targeted lipoplexes containing plasmid DNA coding for GPF. (**a**, **c**, **e**, and **g**) Green filter; (**b**, **d**, **f**, and **h**) red filter; (**i**) merged view of **e** and **f**. Green represents GFP-positive cells, red represents extracellular vWF. At least two independent experiments were performed for each set of conditions. The results relating to two vessels under each of the conditions are shown. Original magnification: ×200. EC, endothelial cell layer; SMC, smooth muscle cell layer.

vessels perfused with VEGF and incubated with the targeted complexes. In these latter vessels, endothelial cell labeling was clearly visible as bright red fluorescence along the length of the artery (**Figure 7h**).

Even with normal fluorescent microscopy it was possible to take fluorescent micrographs of different sections of the artery along the *z*-axis (*i.e.*, top, middle and bottom section; pictures from top and bottom sections not shown), thereby clearly demonstrating the three-dimensional nature of the model.

CXCR4-targeted lipoplexes transfect endothelial cells in mesenteric arteries

Receptor-mediated transfection of mesenteric endothelial cells was tested using a GFP expression plasmid. For the purpose of distinguishing between the endothelial cell layer and the smooth muscle cell layer, the endothelial cells were labeled with von Willebrand factor, a factor constitutively produced in endothelium.[27] The protocol used for immunohistochemical staining did not include a permeabilization step, so that only the von Willebrand factor associated with extracellular matrix is stained (**Figure 8**). In blood vessels that had not been incubated with rrVEGF164 (**Figure 8a–d**), no GFP positive cells were detected following intra-luminal administration of peptide-targeted lipoplexes (**Figure 8a** and **c**). In VEGF-treated vessels (**Figure 8e,f** and **g,h**), perfusion of peptide-targeted lipoplexes resulted in production of GFP-positive endothelial cells, as shown in **Figure 8e** and **g**. Only the cells of the endothelial cell-layer were transfected. No GFP-positive smooth muscle cells were observed (**Figure 8i**). The infusion of non-targeted lipoplexes into untreated or VEGF-treated vessels did not yield any GFP-positive cells (data not shown).

DISCUSSION

Ever since the first gene therapy clinical trial in 1989, in which Rosenberg *et al.* used *ex vivo* gene therapy with retroviruses to treat metastatic melanomas, it has become clear that clinical success depends upon several variables, one of the most

important being the gene delivery system.[28] This dictates the type of cell to which the therapeutic genes are transferred, the expression level of the therapeutic gene, and the duration of expression. The addition of targeting ligands to the surface of gene delivery systems has been an attractive approach to establish improved and more specific gene transfer to cells that express the targeted receptor. A major advantage of cationic lipid-based gene delivery systems as compared to viral systems is the relative ease with which these kinds of targeting ligands are accommodated on their surface with little effect on manufacturing. Changes in viral tropism have also been achieved,[29–32] but these modifications involve alteration of viral structural proteins, and can negatively affect the viral titer.

The lipoplexes described in this report are engineered to target proliferating endothelial cells in tumor vasculature with the aim of treating distant tumors, because these cells will be readily available to the gene delivery system.[3,6] The binding affinity of the ligand for its receptor is of major importance, because the lipoplex will not only have to recognize and bind to the targeted receptor, but will also have to compete with endogenous ligands for the target receptor. The challenge is to identify ligands that have sufficiently high affinity for their targets, and to identify cell surface receptors that are either unique or display increased surface density on the targeted tissue. An interesting example of the importance of receptor density on target cells has been reported by Park *et al.*[33] Their work has shown that anti-ERB2-targeted liposomal doxorubicin readily accumulated in cells that expressed 10^5 or more receptors per cell, leading to a therapeutic effect, but not in cells that expressed only 10^4 receptors per cell. On the basis of these parameters, the chemokine receptor CXCR4 was selected as a receptor to be targeted for tumor-vasculature-specific delivery. The results presented herein show that CXCR4 is overexpressed on endothelial cells in culture, and also on endothelial cells in the context of an intact mesenteric artery, when stimulated with VEGF. This growth factor is abundantly expressed by a large percentage of solid tumors including brain tumors.[34–36] Studies measuring VEGF concentrations in endocavitary fluids of 45 glioma-patients have shown VEGF-levels of 90.9 ± 24.789 ng/ml, the same range that we used in our *in vitro* studies (20–100 ng/ml).[37] Given these findings, it is anticipated that CXCR4-expression is induced in brain tumor vasculature *in vivo*. It is conceivable that only VEGF-stimulated endothelial cells express CXCR4 in numbers that are high enough to overcome the threshold. This has been observed for ERB2-targeted liposomes, and the results from our *in vitro* study with HUVECs and with blood vessel organ culture also support this hypothesis. Moreover, CXCR4 is highly expressed in rat glioma cells (RG2s, data not shown), and therefore CXCR4-targeted complexes would not only bind to proliferating endothelial cells more efficiently, but also to glioma cells, possibly leading to an even more profound anti-tumor effect. CXCR4 expression is also observed on stem cells, myeloid cells, and lymphocytes.[38] However our study clearly shows that specific delivery depends upon the cell-surface density of the receptor and the ligand density on the particle, which can be optimized for specific delivery to target tissue.

The lipoplexes presented in this research study are targeted with a ligand of relatively small molecular weight (4F-benzoyl-TE14011, a peptide-analog consisting of 14 amino acids). There are several advantages in using short peptides rather than antibodies or intact proteins. First, the only structural element in the ligand that we used is the disulfide bond between cysteines 4 and 13. In the case of intact proteins and antibodies, the secondary structure is of crucial importance for retaining specificity and high affinity. Second, most endogenous proteins and antibodies have more then one lysine residue in their primary structure. Coupling such ligands to lipid anchors through reaction of their primary amines with SATA will most likely result in the modification of multiple amines, thereby increasing the probability of affecting the binding affinity to the receptor, and producing heterogeneous derivatization between various protein molecules. 4F-benzoyl-TE14011 has only one lysine (Lys7) which will be modified with SATA. The fact that we see receptor-mediated binding of liposomes which are targeted with the SATA-modified peptide indicates that modification of that single lysine does not affect binding to CXCR4. Third, there is a potential problem in using endogenous proteins or antibodies as targeting ligands, namely, the risk of developing neutralizing antibodies and forming immune complexes (even after humanization).[39] By contrast, even when the peptide 4F-benzoyl-TE14011 and its analogs have been administered systemically, neutralizing antibodies have not been observed to date. This makes the peptide a good candidate for *in vivo* use (N. Fujii, unpublished results). Yet another major advantage of using peptide ligands is that the binding affinity of lead compounds can be optimized by substituting different amino-acids and head groups. This will be especially important if the targeting ligand has to compete with the endogenous ligand for receptor occupancy. 4F-benzoyl-TE14011 possesses a K_d of 1.46 nmol/l (estimated using the method of Cheng and Prusoff[40]), as compared to a K_d of 4.5 nmol/l for CXCL12, the endogenous ligand.[24,41] The threefold difference in binding affinity favors binding of the modeled ligand, especially because 4F-benzoyl-TE14011 is presented in the context of a multivalent ligand in the lipoplex. Multivalent ligands are hypothesized to result in increased binding affinity. Also, the high-affinity ligand does get internalized after coupling to the receptor, but without agonist activity. This is important when targeting CXCR4 in the treatment of solid tumors, because it is undesirable to exert an agonist effect on the receptor.

In summary, the results presented herein show that lipid-based transfection complexes can be specifically targeted to cells that express the CXC-receptor 4 (*e.g.*, proliferating endothelial cells and tumor cells), by using peptides with high binding affinity to the CXCR4-receptor. Specifically, the incorporation of CXCR4 lipopeptide into the lipoplexes enhances the transfection-efficiency ~1.2- to 2.5-fold in RG2s, depending on the mole percentage of the lipopeptide. This is in sharp contrast to the outcome after the introduction of control lipids (*i.e.*, DOPE-Cys and DOPE) into the lipoplex, which renders the transfection complexes less active. When the mole percentage of lipopeptide is maintained at 10% and the DNA dose is varied, CXCR4-targeted complexes transfect RG2s more efficiently at all dosages. Specifically, the same percentage of GFP-positive cells can be seen at a fivefold lower DNA dose (40% GFP-positive at 1 μg/100,000 cells for untargeted complexes versus 0.2 μg for CXCR4-targeted complexes). At 1 μg DNA concentration, the amount of luciferase per well is 20-fold higher with CXCR4-targeted complexes than with untargeted lipoplexes.

Receptor surface expression can be induced by pathologically relevant VEGF concentrations in HUVECs. This observation makes the receptor an interesting target for the use of site-specific gene-delivery, with the specific aim of transfecting proliferating vasculature. Targeted liposomes are able to bind only to those endothelial cells in culture that are induced to express CXCR4. The developed targeted lipoplex can be of high value for the delivery of therapeutic genes to tumor vasculature, various solid tumors, and other tissues that express the receptor in great numbers. Furthermore the mesenteric artery organ culture has been shown to be a biologically relevant model in which results relating to *in vitro* receptor expression, liposome binding, and transfection have been validated. The system also allows for the study of cerebral arteries, because unbranched arteries that are long enough to be mounted between the cannulas can be isolated from the rat brain. The endothelial cells of the intact rat mesenteric arteries also express CXCR4 only after perfusion with VEGF. As a result, lipoplexes with 20 mol% CXCR4-lipopeptide bind to endothelial cells only after stimulation with VEGF. GFP transfection with CXCR4-targeted lipoplexes is greatly enhanced in arteries treated with VEGF, as compared to those not treated with VEGF.

Using various cell lines and a blood vessel organ culture, this system has been shown to work well *in vitro*, and is a promising candidate for *in vivo* studies dealing with the targeting of proliferating endothelium and glioma cells.

MATERIALS AND METHODS

Cell cultures and reagents. The rat glioma 2 (RG2) cell line (American type culture collection, Manassas, VA) was maintained in Dulbecco's modified Eagle's medium with 4 mmol/l L-glutamine adjusted to contain 1.5 g/l sodium bicarbonate and 4.5 g/l glucose, 10% fetal bovine serum and 10% PenStrep (Cellgro, Antioch, IL) at 37 °C and 5% CO_2. The HUVECs were maintained in EGM-1 Bulletkit medium composed of endothelial cell basal medium-1 supplemented with ascorbic acid, fetal bovine serum, hydrocortisone, human epidermal growth factor, gentamycin sulfate (GA-1000), and heparin, as described by the manufacturer (Cambrex, Walkersville, MD) at 37 °C and 5% CO_2. HUVECs were not used after passage 10. The cells were cultured and maintained in a 75-cm^2 flask (Nunc, Rochester, NY). One day before the experiment the cells were washed with 1 ml of trypsin–EDTA (Cellgro, Antioch, IL), removed from the flask with 2 ml of trypsin–EDTA, and plated in 6- or 24-well plates (Nunc, Rochester, NY) at a density of 0.5×10^6 or 0.05×10^6 cells per well, respectively.

Flow cytometry. Cells were grown in 6-well plates in media with and without recombinant rat VEGF-164 (rrVEGF164, R&D systems, Minneapolis, MN), and removed from the plate with a cell-dissociation solution (Mediatech, Herndon, VA). After the cells were washed with phosphate-buffered saline (PBS) containing 1% bovine serum albumin and 0.1% sodium azide they were incubated with 10 µg primary antibody (anti-rat CXCR4 polyclonal; Torrey Pines Biolabs, Houston, TX.) in PBS with 1% bovine serum albumin and 0.1% sodium azide on ice for 30 minutes. Negative control antibodies consisted of appropriately matched isotypes at the same concentrations as primary antibodies. The cells were washed twice with cold PBS containing 1% bovine serum albumin and 0.1% sodium azide and incubated with 20 µg secondary antibodies conjugated to fluorescein-5-isothiocyanate (Jackson Immunoresearch, West Grove, PA) on ice for 30 minutes. After two more washes, the cells were analyzed on the FACSort (BD Biosciences, San Jose, CA). The cells were gated using forward and side scatter dot plotting to exclude debris. The intensity of fluorescence was determined for 10,000 cells. Histograms recorded for gated cells were analyzed using WINMDI 2.8 software (J. Trotter; http://facs.scripps.edu). The percentage of gated cells was compared to that in an isotype antibody control.

Derivatization of peptide to phospholipid. 4-F-Benzoyl-TE140.11 (ref. 23) was kindly provided by N.F. and H.T. The targeting ligand was incorporated into lipid-based vesicles by coupling the peptide covalently to 1,2-Dioleoyl-*sn*-Glycero-3-Phosphoethanolamine-*N*-[4-(*p*-maleimido phenyl)butyramide] (DOPE-MPB). Briefly, the peptide was reacted with a 20-fold molar excess of SATA (Pierce, Rockford, IL) in 70% ethanol at pH = 7.6. Derivatization was confirmed using the fluorescamine assay for primary amines. Briefly, to peptide in solution 0.5 ml of fluorescamine in acetone (0.3 mg/ml) was added. After 10 minutes, fluorescence was measured at λ_{ex} = 390 nm and λ_{em} = 475 nm to confirm loss of the reactive amine (lysine 7). The modified peptide now contained a protected sulfhydryl group that was deprotected using a deprotection solution containing an excess of hydroxylamine (0.5 mol/l hydroxylamine, 0.5 mol/l (*N*-[2-hydroxyethyl]piperazine-NV-[2-ethanesulfonic acid]) (HEPES), 25 mmol/l EDTA, pH = 7.4). After deprotection, the reactive thiol was reacted with equimolar amounts of DOPE-MPB to form a stable thio-ether. The progress of the reaction was monitored by thin layer chromatography. The normal phase plate was run in $CHCl_3$:MeOH:H_2O 65:25:4, and after the reaction was complete the lipopeptide was purified using a double extraction as described by Folch.[42]

Cell-associated fluorescence measurement. The lipopeptide was incorporated into liposomes at 20 mol%. The other liposome components consisted of 45 mol% 1,2-dioleoyl-*sn*-glycero-3-phosphocholine, 30 mol% cholesterol (CHOL), and 5 mol% 1,2-Dioleoyl-*sn*-Glycero-3-Phosphoethanolamine-*N*-(7-nitro-2-1,3-benzoxadiazol-4-yl) (DOPE-NBD) as a fluorescent marker [all lipids from Avanti Polar Lipids (Birmingham, AL)]. After a 1-hour incubation of the liposomes with HUVECs, the cells were thoroughly washed with PBS, and cell-associated binding was measured by fluorescence after lysing the cells.

Reporter gene plasmid vectors. For experiments with plasmid DNA encoding for firefly luciferase, pLC0888 was used.[43] For experiments with plasmid encoding for GFP, gWIZ-GFP vector (Gene Therapy Systems, San Diego, CA) was used. The gWIZ-GFP vector was purified using the Qiafilter plasmid purification (Qiagen, Valencia, CA).

Preparation of lipoplexes. The lipid-based transfection reagent (Genzyme lipid 89:Lym-X-Sorb:Vitamin E 10:89:1) was prepared aseptically by mixing 8 µl of Genzyme lipid 89 (1-(N4-Spermine)-2,3-Dilaurylglycerol Carbamate; 25 mg/ml in chloroform or 0.038 µmol/µl) (Genzyme, Cambridge, MA); 7.5 µl Lym-X-Sorb (Lyso-Phosphatidylcholine:Glycerol Monooleate:Oleic Acid 1:4:2; 138 mg/ml in chloroform or 0.365 µmol/µl) (Avanti Polar Lipids, Alabaster, AL); and 2.2 µl Vitamin E (5.905 mg/ml or 0.0137 µmol/µl) (Sigma, St. Louis, MO), in a clean reagent tube. Once the lipids were thoroughly mixed, the solvent was evaporated using argon. The residual solvent was removed by placing the vial under vacuum in the desiccator for 30 minutes. The dried lipid film was hydrated with 3 ml of HEPES buffered saline (7.5 mmol/l HEPES, 150 mmol/l NaCl). After hydration, the transfection mixture was bath-sonicated for 5 minutes. For experiments with fluorescently tagged lipoplexes, 0.1% Lym-X-Sorb was switched out for 1,2-dioleoyl-*sn*-glycero-3-phosphoethanolamine-*N*-(Lissamine Rhodamine B Sulfonyl) (DOPE-Rhodamine). For experiments with targeted complexes, Lym-X-Sorb was switched out for purified lipopeptide prepared as described above.

Transfections. For transfection, 3 µg of DNA was brought up to a volume of 180 µl with HEPES buffered saline, and 180 µl of transfection reagent was added. This resulted in a lipid:DNA molar ratio of 2. The cells were washed with serum-free RG2 medium. After DNA/Lipid complexation

was complete (~15 minutes), 3 ml of serum-free medium was added to the DNA/Lipid mixture, and 1 ml of diluted transfection-complex was added to each well [(DNA) = 1 μg per well]. After a 3-hour incubation, serum-free medium was replaced with full medium.

Luciferase-assay. Forty-eight hours after transfection, the cells were removed from the incubator and washed with Dulbecco's PBS (DPBS) without calcium and magnesium (Cellgro, Antioch, IL). 150 μl of lysisbuffer (0.1 mol/l potassium phosphate buffer; 1% Tx-100; 1 mmol/l dithiothreitol; 2 mmol/l EDTA; pH = 7.8) (Sigma, St. Louis, MO) was added to each well, and the plate was stored at −80 °C for 10 minutes or until ready to be assayed. The cell lysate was thawed at room temperature and transferred to microfuge tubes. The cell lysate was centrifuged at 13,200 rpm for 5 minutes. Forty microlilters of cell lysate was added to each well of the assay-plate (Whatman, Clifton, NJ). One-hundred microlilter substrate-buffer (30 mmol/l tricine; 3 mmol/l ATP; 15 mmol/l MgSO4; 10 mmol/l dithiothreitol; pH 7.8) and 100 μl of 1 mmol/l D-luciferin pH = 6.2 (Sigma, St. Louis, MO) were added to each well, and the plate was run on a luminometer (Dynex Technologies, West Sussex, UK). A standard curve of recombinant luciferase diluted in lysis buffer was run simultaneously where 100 ng of recombinant luciferase corresponded to 0.5×10^6 relative light units.

All results were normalized to total cell protein by measuring the protein concentrations of all cell lysates using the bicinchoninic acid assay (Pierce, Rockford, IL).

Blood vessel organ culture. Animal-procedures were carried out under the approval of the local committee for animal experiments. Sprague Dawley rats were killed by inhalation of an overdose of isoflurane. The mesentery was dissected and placed in ice-cold DPBS-buffer. Mesenteric artery segments of ~10-mm length were dissected and mounted in an organ culture system.

The CXCR4 expression on cells in the blood vessel organ culture was determined by means of indirect immunohistochemistry. Briefly, after incubating the arteries with medium supplemented with 100 ng/ml rrVEGF164 overnight, 10 μg rabbit anti-rat CXCR4 polyclonal antibody was perfused through the artery in a volume of 1 ml DPBS, and incubated for 30 minutes. After the luminal side of the artery was washed by perfusing 1 ml cold DPBS through the arteries, 20 μg goat anti-rabbit secondary antibody conjugated to fluorescein-5-isothiocyanate (Jackson Immunoresearch, West Grove, PA) was also perfused, and incubated for 30 minutes. After washing the arteries, fluorescent micrographs were taken.

For the experiments with the fluorescent-labeled transfection complexes, empty plasmid DNA was complexed with the transfection reagent and diluted up to 1 ml with medium. This 1 ml was perfused slowly through the arteries and washed with 3 ml of DPBS after a 30-minute incubation. After washing, fluorescent micrographs were taken.

For the vessel transfection experiments, lipoplexes expressing GFP were prepared, 1 μg of DNA was perfused in a volume of 1 ml, and after 3 hours the arteries were washed with DPBS. Reporter gene expression was assessed after 48 hours.

ACKNOWLEDGMENTS

We thank Harm Knot and Yagna Jarajapu for sharing their expertise in blood vessel organ culture, Neil Benson from the ICBR Flow Cytometry Core at the University of Florida for his help with flow cytometry, Alfred Chung for advice on peptide conjugation, and Isamu Ito and David Taylor for their technical assistance and advice. This work was supported in part by a grant from the James S. McDonnell Foundation and a State of Florida Bankhead-Cooley Cancer Research grant. All the lipids that were used were kindly provided by Avanti Polar Lipids.

REFERENCES

1. Templeton, NS, Lasic, DD, Frederik, PM, Strey, HH, Roberts, DD and Pavlakis, GN (1997). Improved DNA: liposome complexes for increased systemic delivery and gene expression. *Nat Biotechnol* **15**: 647–652.
2. Liu, F, Qi, H, Huang, L and Liu, D (1997). Factors controlling the efficiency of cationic lipid-mediated transfection *in vivo* via intravenous administration. *Gene Ther* **4**: 517–523.
3. Holland, HE, Nagy, D, Liu, JJ, Spratt, K, Lee, YL, Danos, O *et al.* (1997). *In vivo* gene transfer by intravenous administration of stable cationic lipid/DNA complex. *Pharm Res* **14**: 742–749.
4. Nicolazzi, C, Mignet, N, de la Figuera, N, Cadet, M, Ibad, RT, Seguin, J *et al.* (2003). Anionic polyethyleneglycol lipids added to cationic lipoplexes increase their plasmatic circulation time. *J Control Release* **88**: 429–443.
5. Anwer, K, Kao, G, Proctor, B, Rolland, A and Sullivan, S (2000). Optimization of cationic lipid/DNA complexes for systemic gene transfer to tumor lesions. *J Drug Target* **8**: 125–135.
6. Anwer, K, Meaney, C, Kao, G, Hussain, N, Shelvin, R, Earls, RM *et al.* (2000). Cationic lipid-based delivery system for systemic cancer gene therapy. *Cancer Gene Ther* **7**: 1156–1164.
7. Liu, Y, Thor, A, Shtivelman, E, Cao, Y, Tu, G, Heath, TD *et al.* (1999). Systemic gene delivery expands the repertoire of effective antiangiogenic agents. *J Biol Chem* **274**: 13338–13344.
8. Wagner, E, Culmsee, C and Boeckle, S (2005). Targeting of polyplexes: toward synthetic virus vector systems. *Adv Genet* **53PA**: 333–354.
9. Yu, JH and Schaffer, DV (2005). Advanced targeting strategies for murine retroviral and adeno-associated viral vectors. *Adv Biochem Eng Biotechnol* **99**: 147–167.
10. Hashida, M, Kawakami, S and Yamashita, F (2005). Lipid carrier systems for targeted drug and gene delivery. *Chem Pharm Bull (Tokyo)* **53**: 871–880.
11. Thomas, M and Klibanov, AM (2003). Non-viral gene therapy: polycation-mediated DNA delivery. *Appl Microbiol Biotechnol* **62**: 27–34.
12. Zhdanov, RI, Podobed, OV and Vlassov, VV (2002). Cationic lipid-DNA complexes-lipoplexes-for gene transfer and therapy. *Bioelectrochemistry* **58**: 53–64.
13. Pardridge, WM (1986). Receptor-mediated peptide transport through the blood-brain barrier. *Endocr Rev* **7**: 314–330.
14. Wu, GY, Wilson, JM, Shalaby, F, Grossman, M, Shafritz, DA and Wu, CH (1991). Receptor-mediated gene delivery *in vivo*. Partial correction of genetic analbuminemia in Nagase rats. *J Biol Chem* **266**: 14338–14342.
15. Wilson, JM, Grossman, M, Wu, CH, Chowdhury, NR, Wu, GY and Chowdhury, JR (1992). Hepatocyte-directed gene transfer *in vivo* leads to transient improvement of hypercholesterolemia in low density lipoprotein receptor-deficient rabbits. *J Biol Chem* **267**: 963–967.
16. Hood, JD, Bednarski, M, Frausto, R, Guccione, S, Reisfeld, RA, Xiang, R *et al.* (2002). Tumor regression by targeted gene delivery to the neovasculature. *Science* **296**: 2404–2407.
17. Ruoslahti, E and Rajotte, D (2000). An address system in the vasculature of normal tissues and tumors. *Annu Rev Immunol* **18**: 813–827.
18. Anwer, K, Kao, G, Rolland, A, Driessen, WH and Sullivan, SM (2004). Peptide-mediated gene transfer of cationic lipid/plasmid DNA complexes to endothelial cells. *J Drug Target* **12**: 215–221.
19. Temming, K, Schiffelers, RM, Molema, G and Kok, RJ (2005). RGD-based strategies for selective delivery of therapeutics and imaging agents to the tumour vasculature. *Drug Resist Updat* **8**: 381–402.
20. Nagasawa, T, Hirota, S, Tachibana, K, Takakura, N, Nishikawa, S, Kitamura, Y *et al.* (1996). Defects of B-cell lymphopoiesis and bone-marrow myelopoiesis in mice lacking the CXC chemokine PBSF/SDF-1. *Nature* **382**: 635–638.
21. Salcedo, R and Oppenheim, JJ (2003). Role of chemokines in angiogenesis: CXCL12/SDF-1 and CXCR4 interaction, a key regulator of endothelial cell responses. *Microcirculation* **10**: 359–370.
22. André, F, Soria, JC, Assi, H, Delaloge, S and Spielmann, M (2004). Expression of chemokine receptors by cancer cells. *Bull Cancer* **91**(Suppl 4): S254–S256.
23. Tamamura, H, Hiramatsu, K, Mizumoto, M, Ueda, S, Kusano, S, Terakubo, S *et al.* (2003). Enhancement of the T140-based pharmacophores leads to the development of more potent and bio-stable CXCR4 antagonists. *Org Biomol Chem* **1**: 3663–3669.
24. Tamamura, H, Hiramatsu, K, Kusano, S, Terakubo, S, Yamamoto, N, Trent, JO *et al.* (2003). Synthesis of potent CXCR4 inhibitors possessing low cytotoxicity and improved biostability based on T140 derivatives. *Org Biomol Chem* **1**: 3656–3662.
25. Tamamura, H, Hori, A, Kanzaki, N, Hiramatsu, K, Mizumoto, M, Nakashima, H *et al.* (2003). T140 analogs as CXCR4 antagonists identified as anti-metastatic agents in the treatment of breast cancer. *FEBS Lett* **550**: 79–83.
26. Kucia, M, Reca, R, Miekus, K, Wanzeck, J, Wojakowski, W, Janowska-Wieczorek, A *et al.* (2005). Trafficking of normal stem cells and metastasis of cancer stem cells involve similar mechanisms: pivotal role of the SDF-1-CXCR4 axis. *Stem Cells* **23**: 879–894.
27. Jaffe, EA, Hoyer, LW and Nachman, RL (1974). Synthesis of von Willebrand factor by cultured human endothelial cells. *Proc Natl Acad Sci USA* **71**: 1906–1909.
28. Rosenberg, SA, Aebersold, P, Cornetta, K, Kasid, A, Morgan, RA, Moen, R *et al.* (1990). Gene transfer into humans—immunotherapy of patients with advanced melanoma, using tumor-infiltrating lymphocytes modified by retroviral gene transduction. *N Engl J Med* **323**: 570–578.
29. Krasnykh, V, Dmitriev, I, Mikheeva, G, Miller, CR, Belousova, N and Curiel, DT (1998). Characterization of an adenovirus vector containing a heterologous peptide epitope in the HI loop of the fiber knob. *J Virol* **72**: 1844–1852.
30. Wickham, TJ, Tzeng, E, Shears, LL 2nd, Roelvink, PW, Li, Y, Lee, GM *et al.* (1997). Increased *in vitro* and *in vivo* gene transfer by adenovirus vectors containing chimeric fiber proteins. *J Virol* **71**: 8221–8229.
31. Büning, H, Ried, MU, Perabo, L, Gerner, FM, Huttner, NA, Enssle, J *et al.* (2003). Receptor targeting of adeno-associated virus vectors. *Gene Ther* **10**: 1142–1151.
32. Ried, MU, Girod, A, Leike, K, Büning, H and Hallek, M (2002). Adeno-associated virus capsids displaying immunoglobulin-binding domains permit antibody-mediated vector retargeting to specific cell surface receptors. *J Virol* **76**: 4559–4566.

33. Park, JW, Hong, K, Kirpotin, DB, Colbern, G, Shalaby, R, Baselga, J *et al.* (2002). Anti-HER2 immunoliposomes: enhanced efficacy attributable to targeted delivery. *Clin Cancer Res* **8**: 1172–1181.
34. Toi, M, Kondo, S, Suzuki, H, Yamamoto, Y, Inada, K, Imazawa, T *et al.* (1996). Quantitative analysis of vascular endothelial growth factor in primary breast cancer. *Cancer* **77**: 1101–1106.
35. Sehgal, A, Keener, C, Boynton, AL, Warrick, J and Murphy, GP (1998). CXCR-4, a chemokine receptor, is overexpressed in and required for proliferation of glioblastoma tumor cells. *J Surg Oncol* **69**: 99–104.
36. Müller, A, Homey, B, Soto, H, Ge, N, Catron, D, Buchanan, ME *et al.* (2001). Involvement of chemokine receptors in breast cancer metastasis. *Nature* **410**: 50–56.
37. Salmaggi, A, Eoli, M, Frigerio, S, Silvani, A, Gelati, M, Corsini, E *et al.* (2003). Intracavitary VEGF, bFGF, IL-8, IL-12 levels in primary and recurrent malignant glioma. *J Neurooncol* **62**: 297–303.
38. Bermejo, M, Martín-Serrano, J, Oberlin, E, Pedraza, MA, Serrano, A, Santiago, B *et al.* (1998). Activation of blood T lymphocytes down-regulates CXCR4 expression and interferes with propagation of X4 HIV strains. *Eur J Immunol* **28**: 3192–3204.
39. Dillman, RO (2001). Monoclonal antibodies in the treatment of malignancy: basic concepts and recent developments. *Cancer Invest* **19**: 833–841.
40. Cheng, Y and Prusoff, WH (1973). Relationship between the inhibition constant (K1) and the concentration of inhibitor which causes 50 per cent inhibition (I50) of an enzymatic reaction. *Biochem Pharmacol* **22**: 3099–3108.
41. Di Salvo, J, Koch, GE, Johnson, KE, Blake, AD, Daugherty, BL, DeMartino, JA *et al.* (2000). The CXCR4 agonist ligand stromal derived factor-1 maintains high affinity for receptors in both $G_{\alpha}(i)$-coupled and uncoupled states. *Eur J Pharmacol* **409**: 143–154.
42. Folch, J, Ascoli, I, Lees, M, Meath, JA and LeBaron, N (1951). Preparation of lipide extracts from brain tissue. *J Biol Chem* **191**: 833–841.
43. Li, S, MacLaughlin, FC, Fewell, JG, Li, Y, Mehta, V, French, MF *et al.* (1999). Increased level and duration of expression in muscle by co-expression of a transactivator using plasmid systems. *Gene Ther* **6**: 2005–2011.

Exploratory Studies on Development of the Chemokine Receptor CXCR4 Antagonists Toward Downsizing

Hirokazu Tamamura,[1] Hiroshi Tsutsumi,[1] Wataru Nomura[1] and Nobutaka Fujii[2]

[1]Institute of Biomaterials and Bioengineering, Tokyo Medical and Dental University, Chiyoda-ku, Tokyo 101-0062, Japan. [2]Graduate School of Pharmaceutical Sciences, Kyoto University, Sakyo-ku, Kyoto 606-8501, Japan.

Abstract: Seven transmembrane (7TM) G-protein-coupled receptor (GPCR) families are important targets for drug discovery, and specific antagonists for GPCR can accelerate research in the field of medicinal chemistry. The chemokine receptor CXCR4 is a GPCR that possesses a unique ligand CXCL12/stromal cell-derived factor-1 (SDF-1). The interaction between CXCL12 and CXCR4 is essential for the migration of progenitor cells during embryonic development of the cardiovascular, hemopoietic and central nervous systems, and also involved in several intractable disease processes, including HIV infection, cancer cell metastasis, progression of acute and chronic leukemias, rheumatoid arthritis and pulmonary fibrosis. Thus, CXCR4 may be an important therapeutic target in all of these diseases, and various CXCR4 antagonists have been proposed as potential drugs. Fourteen-mer peptides, T140 and its analogs, and downsized cyclic pentapeptides have been developed by us as potent CXCR4 antagonists. This article describes the development of a number of specific CXCR4 antagonists in our laboratory, including downsizing.

Keywords: cancer metastasis, chemokine receptor, CXCR4 antagonist, downsizing, HIV infection, rheumatoid arthritis

Introduction

As a postgenome project, proteomics has been prosperous in life science, and selective ligands involving protein networks have been valuable and useful for studies on chemical biology. Seven transmembrane G-protein-coupled receptors (7TM-GPCRs) are great targets for drug discovery and chemical biology. Thus, development of selective antagonists against each GPCR is extremely desirable (Tamamura and Tsutsumi, 2006). Chemokines are a chemotactic cytokine family that induces migration of leukocytes. Receptors of chemokines, which transduce signals of the corresponding chemokines, are classified into GPCR families. The relationships between chemokines and their receptors are highly interconnected and complicated: in most cases, a single chemokine recognizes a plurality of receptors, and one chemokine receptor recognizes several chemokines. Thus, most of chemokines lack receptor selectivity. However, the chemokine CXCL12/stromal cell-derived factor-1 (SDF-1) possesses the chemokine receptor CXCR4 as its solitary receptor (Tashiro et al. 1993; Nagasawa, Kikutani and Kishimoto, 1994; Oberlin et al. 1996; Bleul et al. 1996). The interaction between CXCL12 and CXCR4 plays a fundamental role in the migration of progenitor cells during embryonic development of the hemopoietic, intestine vascular, cardiovascular and central nervous systems. Its physiological roles in adults remain poorly disclosed. It is also known that the CXCR4-CXCL12 pair is involved in various disease processes such as HIV infection (Feng et al. 1996), cancer cell metastasis (Koshiba et al. 2000; Geminder et al. 2001; Müller et al. 2001; Robledo et al. 2001; Sanz-Rodriguez, Hidalgo and Teixido, 2001; Scotton et al. 2001; Bertolini et al. 2002; Kijima et al. 2002; Schrader et al. 2002; Scotton et al. 2002; Taichman et al. 2002; Burger et al. 2003; Rubin et al. 2003; Tamamura, Hori et al. 2003; Takenaga et al. 2004; Mori et al. 2004; Piovan et al. 2005; Zannettino et al. 2005), progression of acute and chronic leukemias (Tsukada et al. 2002; Juarez et al. 2003; Burger et al. 2005; Spoo et al. 2007) and rheumatoid arthritis (Nanki et al. 2000) (Fig. 1).

CXCR4 was initially identified as a second receptor (co-receptor) of T cell line-tropic (X4-) HIV-1 entry through its association with the first receptor, CD4. Macrophage-tropic (R5-) HIV-1 strains, which use the chemokine receptor CCR5 as another co-receptor, are major in early stages of HIV infection

Correspondence: Hirokazu Tamamura, Tel: 81-3-5280-8036; Email: tamamura.mr@tmd.ac.jp

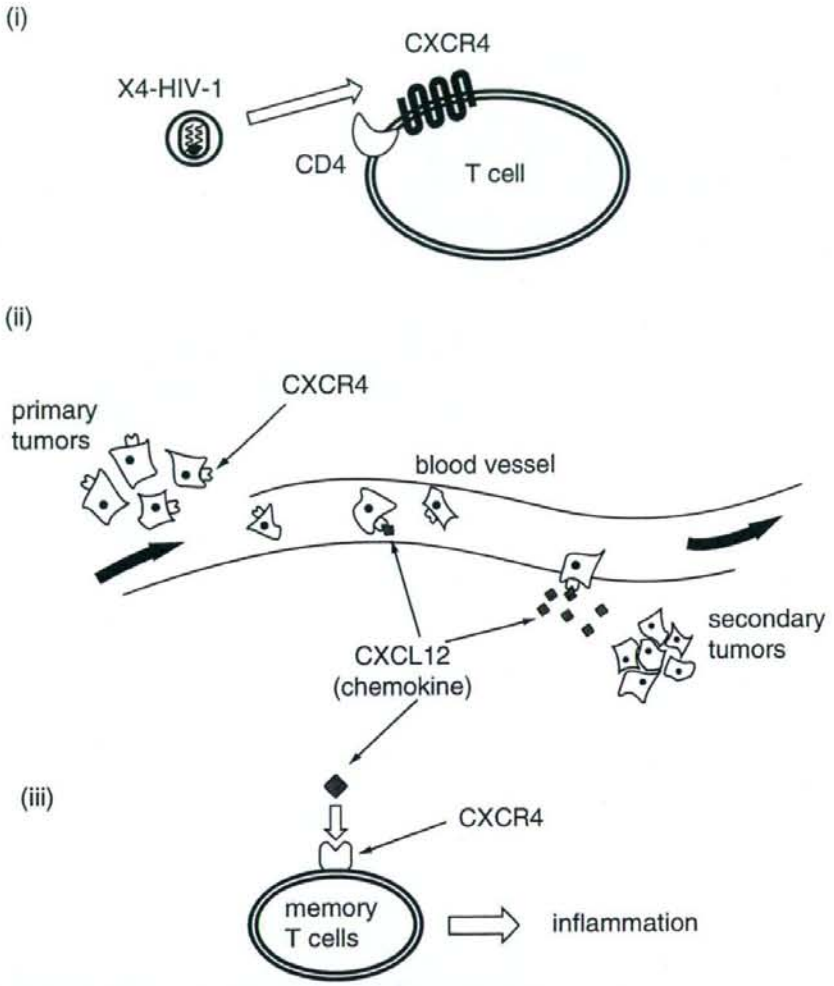

Figure 1. Various disorders relevant to the CXCL12-CXCR4 axis, such as HIV infection (i), cancer cell metastasis (ii) and rheumatoid arthritis (iii).

(Alkhatib et al. 1996; Choe et al. 1996; Deng et al. 1996; Doranz et al. 1996; Dragic et al. 1996). However, X4 HIV-1 strains become dominant in the late stages. Recently, it has also been reported that CXCL12 is highly expressed in several internal organs that are the primary targets of cancer cell metastasis, and that CXCR4 is overexpressed on the surfaces of several types of cancer cells. Thus, it has been shown that the CXCL12-CXCR4 axis is associated to metastasis of several types of cancer including cancer of the pancreas, breast, lung, kidney, and prostate and non-Hodgkin's lymphoma, neuroblastoma, melanoma, ovarian cancer, multiple myeloma and malignant brain tumors. Furthermore, this axis is also correlated to the progression of chronic lymphocytic leukemia (CLL) and acute lymphoblastic leukemia (ALL), and acute myeloid leukemia (AML). In addition, rheumatoid arthritis (RA) is caused mainly by $CD4^+$ memory T cell accumulation in the inflamed synovium. It was reported that CXCL12 concentration is extremely elevated in the synovium of RA

patients, and that CXCR4 is highly expressed on the surface of memory T cells. Further, CXCL12 stimulates migration of the memory T cells and thereby inhibits T cell apoptosis. This indicates that the CXCR4-CXCL12 interaction plays an essential role in the accumulation of T cells in the RA synovium. Taken together, CXCR4 is an attractive therapeutic target for these diseases, and our recent research concerning the development of several CXCR4 antagonists including downsizing is discussed in this review article.

Development of CXCR4 Antagonists as Selective Inhibitors of X4-HIV-1 Entry

Self-defense peptides with antibacterial and antiviral activities, tachyplesins and polyphemusins, have been isolated from the hemocyte debris of the Japanese horseshoe crab (*Tachypleus tridentatus*) and the American horseshoe crab (*Limulus polyphemus*), which are 17-mer and 18-mer peptides, respectively (Fig. 2) (Nakamura et al. 1988; Miyata et al. 1989). Our preliminary structure-activity relationship studies of these peptides led to the development of T22 ([$Tyr^{5,12}$, Lys^{7}]-polyphemusin II) (Masuda et al. 1992; Nakashima et al. 1992) and its downsized 14-mer peptide, T140, which possess strong anti-HIV activity (Fig. 2) (Tamamura et al. 1998). T22 and T140 effectively block X4-HIV-1 entry into cells by binding specifically to CXCR4, and inhibit Ca^{2+} mobilization caused by CXCL12 stimulation against CXCR4 (Murakami et al. 1997; Xu et al. 1999; Murakami et al. 1999). In addition, a T140 analog exhibited a remarkable and significant delaying of the appearance of drug-resistant strains of HIV in passage experiments using cell cultures *in vitro* (Kanbara et al. 2001), and it was presumed that the T140 analogs would be useful for its suppressive effect against drug-resistant strains. Structural analysis revealed that T140 forms an antiparallel β-sheet structure supported by a disulfide bridge between Cys^{4} and Cys^{13}, which is connected by a type II' β-turn (Tamamura, Sugioka et al. 2001). Four amino acid residues that were contained in T140, Arg^{2}, L-3-(2-naphthyl)alanine $(Nal)^{3}$, Tyr^{5} and Arg^{14}, were identified as residues indispensable for significant activity (Tamamura et al. 2000).

However, T140 is proven to be biologically unstable, and biodegradable in mouse/feline serum or in rat liver homogenate (Tamamura, Omagari et al. 2001; Tamamura, Hiramatsu, Kusano et al. 2003). When indispensable amino acid residues (Arg^{14} in serum; Arg^{2}, Nal^{3} and Arg^{14} in liver homogenate) are deleted from the *N*- and the *C*-termini, the efficacy of degraded peptides is dramatically reduced. Modification of T140 analogs at both termini efficiently suppresses the above biodegradations and leads to development of novel

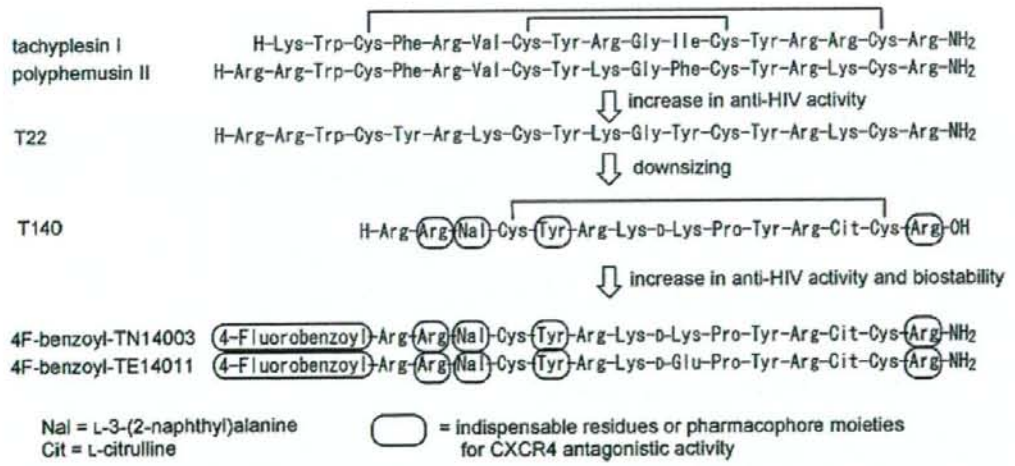

Figure 2. Structures of tachyplesin I, polyphemusin II, its analog T22, its downsized analog T140, its biostable analogs 4F-benzoyl-TN14003 and 4F-benzoyl-TE14011.

and effective compounds that show highly CXCR4-antagonistic activity as well as increased biological stability. Further studies on the *N*-terminal modification found an electron-deficient aromatic ring such as a 4-fluorobenzoyl moiety at the *N*-terminus to constitute a novel pharmacophore for strong anti-HIV activity. The T140 analogs, which contain an *N*-terminal 4-fluorobenzoyl moiety, 4F-benzoyl-TN14003 and 4F-benzoyl-TE14011, have anti-HIV activity two orders of magnitude higher than that of T140 and enhanced biostability in serum/liver homogenates (Fig. 2) (Tamamura, Hiramatsu, Mizumoto et al. 2003).

Cyclic Peptides with CXCR4 Antagonistic Activity Derived from T140

Arg^2, Nal^3, Tyr^5 and Arg^{14} of T140, which are located in close proximity to each other in space, are indispensable to high antagonistic activity against CXCR4 as described above. For downsizing of T140 analogs, a pharmacophore-guided approach was performed using cyclic pentapeptide libraries, which were composed of two L/D-Arg, L/D-Nal and L/D-Tyr in addition to Gly as a spacer. This approach led to FC131 [*cyclo*(-Arg^1-Arg^2-Nal^3-Gly^4-D-Tyr^5-)], which showed strong CXCR4-antagonistic activity comparable to that of T140 (Fig. 3) (Fujii et al. 2003). Structural analysis of FC131 by NMR and simulated annealing molecular dynamics revealed the near-symmetrical pentagonal backbone structure.

A 4-fluorophenyl moiety found as a pharmacophoric moiety as described in the above section was introduced into cyclic pentapeptides. Since replacement of the phenol group of D-Tyr^5 by a 4-fluorophenyl group did not cause the maintenance of high potency, the 4-fluorophenyl group

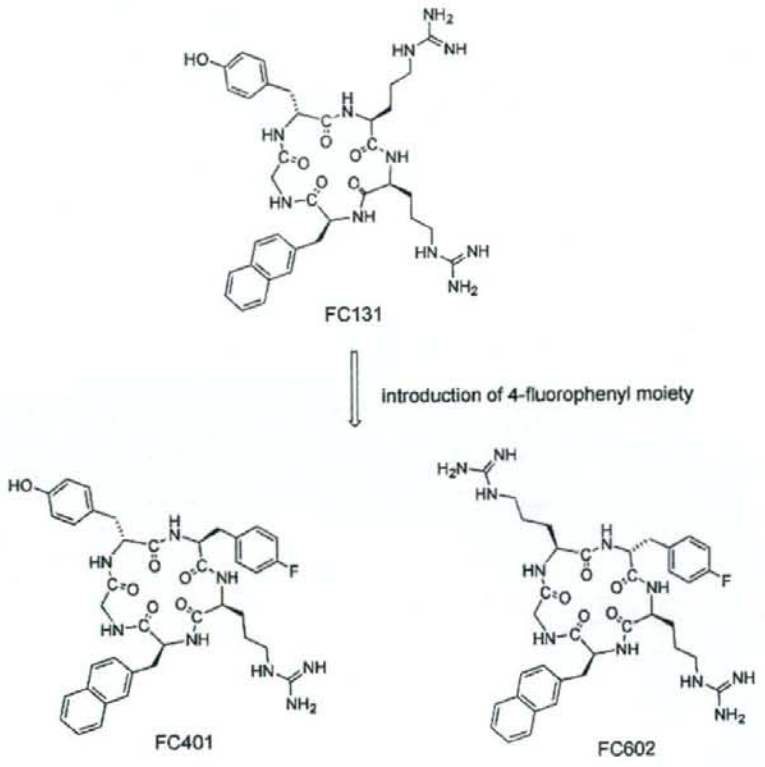

Figure 3. Structures of cyclic pentapetides FC131, FC401 and FC602.

was incorporated into position 1. The resulting compound, FC401 ([Phe(4-F)^1]-FC131), shows significant CXCR4-binding activity (Fig. 3) (Tamamura et al. 2005). Next, since a second Arg residue is thought to be indispensable for high potency and an aromatic residue [L/D-Phe(4-F)] has been incorporated into position 1, four analogs [L/D-Phe(4-F)^1, L/D-Arg^5]-FC131 were synthesized based on replacement of D-Tyr^5 by L/D-Arg^5. Among these analogs, FC602, which is [D-Phe(4-F)^1, Arg^5]-FC131, shows the most potent activity, which is 10-fold greater than that of [D-Tyr^1, Arg^5]-FC131 (Fig. 3). Thus, FC602 is a novel lead, which involves a pharmacophore moiety different from the pharmacophore groups of FC131.

A Linear Type of Low Molecular Weight CXCR4 Antagonists

Identification of a novel pharmacophore for CXCR4 antagonism, such as a 4-fluorobenzoyl or 4-fluorophenyl moiety, prompted us to develop a linear type of low molecular weight CXCR4 antagonists. By combining substructure units of the T140 pharmacophore and new pharmacophore moieties, several compounds were designed and synthesized using combinatorial chemistry. As a result, several linear compounds were found as moderate CXCR4 antagonists, such as compounds **1–3** shown in Figure 4 (Tamamura, Tsutsumi et al. 2006). These compounds are relatively weaker than a cyclic pentapeptide FC131. Thus, it is thought that conformational constriction based on a cyclic pentapeptide scaffold is critical for strong potency.

Anthracene derivatives possessing two sets of zinc(II)-2,2'-dipicolylamine complex were previously found as useful chemosensors that can selectively bind to phosphorylated peptide surfaces (Ojida et al. 2004). Several low molecular weight compounds bearing the complex structure were identified as selective CXCR4 antagonists (Tamamura, Ojida et al. 2006). Molecular superposition of structures of the zinc(II)-2,2'-dipicolylamine complex compound 4 and the cyclic pentapeptide FC131 was investigated as it provided the best fit with the maintenance of local energy minimizations of both of the structures (Fig. 4). The distance between two dipicolylamine moieties of compound 4 is estimated to be nearly equal to that between the two Arg side chains of FC131. Thus, the distance of these functional groups is thought to be

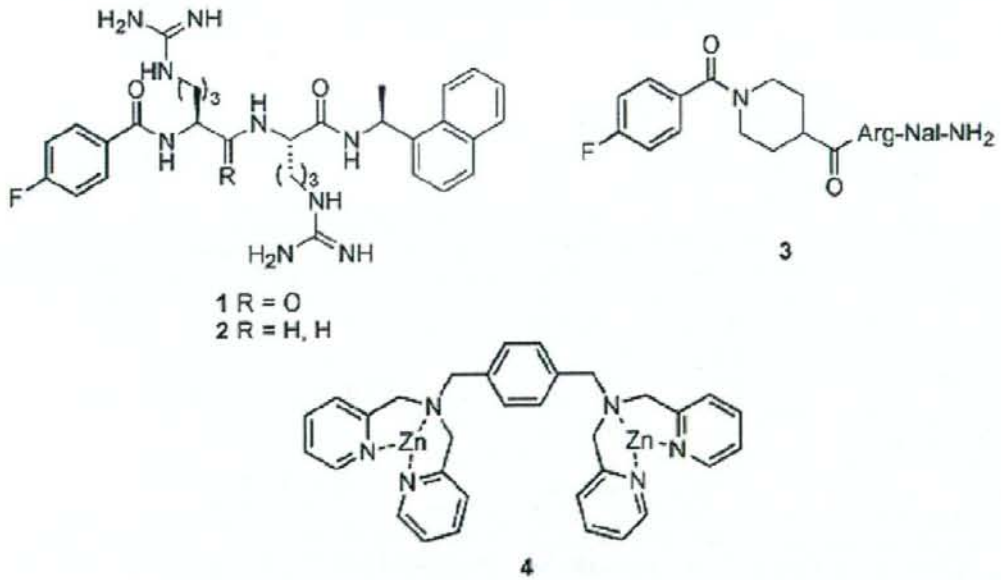

Figure 4. Structures of a linear type of low molecular weight CXCR4 antagonists.

essential for expression of CXCR4 antagonistic activity.

Anti-Metastasis Activity of T140 Analogs Against Breast Cancer, Melanoma and Pancreatic Cancer

While CXCR4 and another chemokine receptor, CCR7, are highly expressed on the surface of human breast cancer cells, CXCL12 and a CCR7 ligand, CCL21, are highly expressed in lymph nodes, bone marrow, lung and liver, which form the common metastatic destinations of breast cancer. The CXCL12-CXCR4/CCR7-CCL12 axis might determine the metastatic destination of tumor cells and cause organ-preferential metastasis (Müller et al. 2001). Metastasis of breast cancer cells to the lung in mice was inhibited by neutralizing CXCR4 with anti-CXCR4 antibodies. We evaluated the inhibitory activity of our T140 analogs against the migration of breast cancer cells *in vitro* and metastasis of breast cancer cells *in vivo* (Tamamura, Hori et al. 2003). T140 analogs inhibited in dose-dependent manners the migration of a CXCR4-positive human breast carcinoma cell line MDA-MB-231 induced by CXCL12. Furthermore, the inhibitory effect of a bio-stable T140 analog, 4F-benzoyl-TN14003, was confirmed using experimental metastasis models of breast cancer, in which MDA-MB-231 cells were injected intravenously into the tail vein of SCID mice and trapped in the lung to which they migrated through the heart and the pulmonary artery. 4F-benzoyl-TN14003 was subcutaneously injected using an Alzet osmotic pump (DURECT Corp., Cupertino, CA, U.S.A.), and an effective suppression of tumor accumulation was then shown on the lung surface as a result of MDA-MB-231 metastasis. This suggests that small molecule CXCR4 antagonists, such as T140 analogs, can replace anti-CXCR4 antibodies as neutralizers of metastasis of breast cancer.

It was reported that an excessive expression of CXCR4 on B16 melanoma cells enhances the metastatic accumulation of the cells in mouse lung, and that a CXCR4 antagonist T22 blocks pulmonary metastasis in mice injected with CXCR4-transduced B16 cells (Murakami et al. 2002). We found that T140 analogs inhibited pulmonary metastasis in mice injected with B16 cells, which are not transduced with CXCR4 (Takenaga et al. 2004). Poly D,L-lactic acid (PLA) microcapsules containing a T140 analog, 4F-benzoyl-TE14011, was subcutaneously injected in experimental metastatic models of CXCR4-positive B16-BL6 melanoma cells. 4F-benzoyl-TE14011 is released in a controlled fashion from the PLA microcapsules for a long period *in vivo* with the maintenance of the level of the 4F-benzoyl-TE14011 concentration in blood. A single subcutaneous administration of 4F-benzoyl-TE14011-PLA significantly decreases the number of colonies ascribed to pulmonary metastasis of B16-BL6 cells. Thus, a controlled release of CXCR4 antagonists might lead to effective suppression of cancer metastasis.

While CXCL12 mRNA is expressed in pancreatic cancer tissues, CXCR4 mRNA is expressed both in pancreatic cancer tissues and in pancreatic cancer cell lines (AsPC-1, BxPC-3, CFPAC-1, HPAC and PANC-1) (Koshiba et al. 2000). CXCL12 stimulates induction of both migration and invasion of pancreatic cancer cells, AsPC-1, PANC-1 and SUIT-2, in dose-dependent manners *in vitro*. Thus, it suggests that the interaction between CXCL12 and CXCR4 is relevant to pancreatic cancer cell progression and metastasis. CXCL12-induced migration and invasion of these cells are suppressed by T140 analogs in dose-dependent manners (Mori et al. 2004). CXCL12 treatment of PANC-1 cells induces a drastic increase in actin polymerization (cytoskeleton), which causes the invasion and subsequent metastasis of malignant cells into tissues. T140 analogs effectively inhibit this phenomenon.

Furthermore, the CXCL12-CXCR4 axis is relevant to metastasis of SCLC and osteolysis in multiple myeloma. Thus, the blockade of this axis might be an effective remedy against these diseases (Hartmann et al. 2005; Zannettino et al. 2005).

CXCR4 is expressed in malignant cells in at least 23 different types of cancer (Balkwill 2004), including those discussed above. Antagonists of CXCR4 such as the T140 analogs might be useful lead compounds for the development of anti-metastatic agents in several types of cancer.

Effect of T140 Analogs Against ALL and CLL

Growth and survival of ALL precursor B (pre-B) cells might be caused by mutual contact with bone marrow stromal layers through adhesive interactions between leukemia cells expressing CXCR4 along with integrins and stromal cells expressing CXCL12 and integrin ligands. Migration of these

cells into stromal layers is stimulated by CXCL12, which is constitutively secreted at high levels by marrow stromal cells, since CXCR4 is highly expressed in the pre-B cells. T140 suppresses CXCL12-induced chemotaxis of the cells and attenuates their migration into bone marrow stromal layers. Furthermore, since T140 analogs enhance the cytotoxic and anti-proliferative effects of other anti-cancer agents such as vincristine and dexamethasone, T140 analogs might overcome cell adhesion-mediated drug resistance (CAM-DR) in ALL chemotherapy (Juarez et al. 2003).

On the other hand, B cell CLL, which is the most frequent leukemia in adults in Western countries, is caused by the accumulation of long-lived, monoclonal, malignant B cells in blood, secondary lymphoid organs and bone marrow. CLL B cells that highly express CXCR4 are activated by CXCL12 released from marrow stromal cells or nurselike cells. CXCL12-stimulation rescues the CLL B cells from apoptosis and contributes to their accumulation. Consequently, the CXCL12-CXCR4 axis should also be a therapeutic target of B cell CLL (Burger et al. 2000). Practically, T140 analogs inhibit chemotaxis of CLL B cells induced by CXCL12, their migration beneath marrow stromal cells and actin polymerization in dose-dependent manners, *in vitro* (Burger et al. 2005). Furthermore, T140 analogs attenuate the anti-apoptotic effect of CXCL12 and prevent stromal cells from protecting against spontaneous apoptosis of CLL B cells. Cocultivation of CLL B cells with marrow stromal cells causes stromal CAM-DR, protecting CLL B cells from undergoing fludarabine-induced apoptosis. Treatment with T140 analogs re-sensitizes these B cells towards fludarabine-induced apoptosis T140 analogs might overcome CAM-DR which is a serious problem in the clinical CLL chemotherapy.

Anti-RA Activity of T140 Analogs

The development of biological drugs such as monoclonal antibodies, which target inflammatory cytokines: tumor necrosis factor, TNF-α, interferon, IFN-γ, the interleukins, IL-1, IL-6, etc., has brought useful results in clinical RA therapy. However, complete curative effects have not yet been achieved. Thus, other drugs, which are not relevant to the functions of these cytokines, are required to improve RA chemotherapy. Since the CXCR4-CXCL12 axis plays a critical role in the accumulation of memory T cells in the RA synovium (Nanki et al. 2000), anti-RA activity of 4F-benzoyl-TN14003 was evaluated. Delayed-type hypersensitivity (DTH) reaction induced by sheep red blood cells (SRBC) was performed as an *in vivo* experimental model of the cellular immune response (Tamamura et al. 2004). Subcutaneous injection of 4F-benzoyl-TN14003 using an Alzet osmotic pump significantly suppressed the footpad swelling (the DTH response) in dose-dependent manners. Collagen-induced arthritis (CIA) in mice was adopted as the other *in vivo* experimental RA model. Several symptoms of arthritis: score increase, body weight loss, ankle swelling, limb weight gain, etc. were remarkably suppressed. Furthermore, the increase in levels of serum anti-bovine CII IgG2a antibody was apparently suppressed in mice treated with 4F-benzoyl-TN14003 subcutaneously using an Alzet osmotic pump after treatment with the bovine type II collagen (CII) emulsion booster. 4F-benzoyl-TN14003 exhibits an inhibitory effect towards the humoral immune response to CII. Thus, CXCR4 antagonists such as T140 analogs might also be useful leads for anti-RA agents.

Other CXCR4 Antagonists

Several low molecular weight CXCR4 antagonists, which are not correlated to T140, have been reported to date (Mastrolorenzo, Scozzafava and Supuran, 2001; Scozzafava, Mastrolorenzo and Supuran, 2002). AMD3100 bearing two cyclam groups (Genzyme) (Schols et al. 1997), an *N*-pyridinylmethylene cyclam (monocyclam) AMD3465 (Genzyme) (De Clercq, 2002), AMD8665 without a cyclam group (Genzyme) (Seibert and Sakmar, 2004), AMD070 (Genzyme) (Vermeire et al. 2004), ALX40-4C (Ac-$[D\text{-}Arg]_9$-NH_2; NPS Allelix) (Doranz et al. 1997), CGP64222 (Cabrera et al. 2002), R3G (Cabrera et al. 2000), NeoR (Daelemans et al. 2000), a distamycin analog, NSC651016 (Howard et al. 1998) and a flavonoid compound, ampelopsin (Liu et al. 2004), have been identified as CXCR4 antagonists. Conjugates of AMD3100 and galactosylceramide (GalCer) analog have also been found as doubly-functionalized drugs (Daoudi et al. 2004). KRH-1636 (Kureha Chemical and Sankyo) is an orally bioavailable agent possessing *N*-pyridinylmethylene, Arg and naphthalene moieties (Ichiyama et al. 2003). A review of non-T140-related CXCR4 antagonists has been published elsewhere (Tamamura and Fujii, 2005).

Conclusion

We have found strong anti-HIV agents, T22 and its downsized analog T140, identified as entry inhibitors that bind specifically to the chemokine receptor CXCR4 and thus inhibit entry of X4-HIV-1 to T-cells. T140 and its analogs also show effective activity against cancer metastasis, leukemia and rheumatoid arthritis. Cyclic pentapeptide FC131 was developed as a new low molecular weight CXCR4 antagonist by downsizing of T140. Furthermore, a linear type of low molecular weight CXCR4 antagonists involving aromatic compounds having the zinc(II)-2,2'-dipicolylamine complex structure have been found. These antagonists might be promising agents for clinical chemotherapy of multiple disorders such as HIV infection, cancer metastasis, leukemia and RA. However, blocking of the CXCL12-CXCR4 axis might be a risky procedure because CXCR4 plays a critical role in embryogenesis, homeostasis and inflammation in the fetus especially in the embryonic development of hemopoietic, cardiovascular and central nervous systems. Use of CXCR4 antagonists combined with CCR5 antagonists/fusion inhibitors might lead to a useful candidate for clinical AIDS chemotherapy.

Acknowledgements

This work was supported in part by a 21st Century COE Program "Knowledge Information Infrastructure for Genome Science", a Grant-in-Aid for Scientific Research from the Ministry of Education, Culture, Sports, Science and Technology, Japan, the Japan Health Science Foundation and The authors wish to acknowledge their collaborators: Profs. Naoki Yamamoto (National Institute of Infectious Diseases/Tokyo Medical and Dental University), Hideki Nakashima (St. Marianna University), Hiroaki Mitsuya (Kumamoto University), Toshio Hattori (Tohoku University), Michinori Waki (Kyushu University), Tsutomu Murakami (National Institute of Infectious Diseases), Ryuichiro Doi (Kyoto University), Masayuki Imamura (Kyoto University), Yuetsu Tanaka (University of the Ryukyus), Akira Otaka (The University of Tokushima), Itaru Hamachi (Kyoto University), Linda J. Bendall (University of Sydney), John O. Trent (University of Louisville) and Stephen C. Peiper (Medical College of Georgia), Drs. Tomohiko Mori (Kyoto University), Mitsuko Takenaga (St. Marianna University), Rie Igarashi, (St. Marianna University), Zixuan Wang (Medical College of Georgia), Jan A. Burger (Freiburg University), Meike Burger (Freiburg University), Andrew C. W. Zannettino (University of Adelaide), Erich Piovan (University of Padua), Jason G. Cyster (University of California San Francisco), Jialin Zheng (University of Nebraska Medical Center), Nikolaus Heveker (Universite de Montreal), Huangui Xiong (University of Nebraska Medical Center), Margitta Retz (University of California San Francisco), Shuichi Kusano (St. Marianna University), Shigemi Terakubo (St. Marianna University), Akio Ojida (Kyoto University), Shinya Oishi (Kyoto University), Mr. Kenichi Hiramatsu (Kyoto University), Satoshi Ueda (Kyoto University), Takanobu Araki (Kyoto University), Tomohiro Tanaka (Tokyo Medical and Dental University), Yasuaki Tanabe (Tokyo Medical and Dental University), Ms. Akane Omagari (Kyoto University), Ai Esaka (Kyoto University) and Nami Ohashi (Tokyo Medical and Dental University).

References

Alkhatib G., Combadiere C., Broder C.C., et al. 1996. Science, 272:1955–8.
Balkwill, F. 2004. *Semin. Cancer Biol.*, 14:171–9.
Bertolini, F., Dell'Agnola, C., Mancuso, P. et al. 2002. *Cancer Res.*, 62:3106–12.
Bleul, C.C., Farzan, M., Choe, H. et al. 1996. *Nature*, 382:829–33.
Burger, J.A., Tsukada, N., Burger, M. et al. 2000. *Blood*, 96:2655–63.
Burger, M., Glodek, A., Hartmann, T. et al. 2003. *Oncogene*, 22:8093–101.
Burger, M., Hartmann, T., Krome, M. et al. 2005. *Blood*, 106:1824–30.
Cabrera, C., Gutierrez, A., Barretina, J. et al. 2002. *Antiviral Res.*, 53:1–8.
Cabrera, C., Gutierrez, A., Blanco, J. et al. 2000. *AIDS Res. Hum. Retroviruses*, 16:627–34.
Choe, H., Farzan, M., Sun, Y. et al. 1996. *Cell.*, 85:1135–48.
Daelemans, D., Schols, D., Witvrouw, M. et al. 2000. *Mol. Pharmacol.*, 57:116–24.
Daoudi, J.-M., Greiner, J., Aubertin, A-M. et al. 2004. *Bioorg Med. Chem. Lett.*, 14:495–8.
De Clercq, E. 2002. *Med. Res. Rev.*, 22:531–65.
Deng, H.K., Liu, R., Ellmeier, W. et al. 1996. *Nature*, 381:661–6.
Doranz, B.J., Grovit-Ferbas, K., Sharron, M.P. et al. 1997. *J. Exp. Med.*, 186:1395–400.
Doranz, B.J., Rucker, J., Yi, Y.J. et al. 1996. *Cell.*, 85:1149–58.
Dragic, T., Litwin, V., Allaway, G.P. et al. 1996. *Nature*, 381:667–73.
Feng, Y., Broder, C.C., Kennedy, P.E. et al. 1996. *Science*, 272:872–77.
Fujii, N., Oishi, S., Hiramatsu, K. et al. 2003. *Angew Chem. Int. Ed. Engl.*, 42:3251–3.
Geminder, H., Sagi-Assif, O., Goldberg, L. et al. 2001. *J. Immunol.*, 167:4747–57.
Hartmann, T.N., Burger, J.A., Glodek, A. et al. 2005. *Oncogene*, 24:4462–71.
Howard, OMZ., Oppenheim, J.J., Hollingshead, M.G. et al. 1998. *J. Med. Chem.*, 41:2184–93.
Ichiyama, K., Yokoyama-Kumakura, S., Tanaka, Y. et al. 2003. *Proc. Natl. Acad. Sci. U.S.A.*, 100:4185–90.
Juarez, J., Bradstock, K.F., Gottlieb, D.J. et al. 2003. *Leukemia*, 17:1294–300.

Kanbara, K., Sato, S., Tanuma, J. et al. 2001. *AIDS Res. Hum. Retroviruses*, 17:615–22.
Kijima, T., Maulik, G., Ma, P.C. et al. 2002. *Cancer Res.*, 62:6304–11.
Koshiba, T., Hosotani, R., Miyamoto, Y. et al. 2000. *Clin. Cancer Res.*, 6:3530–5.
Liu, D-Y., Ye, J-T., Yang, W-H. et al. 2004. *Biomed Environ Sci.*, 17:153–64.
Mastrolorenzo, A., Scozzafava, A. and Supuran, C.T. 2001. *Expert Opin. Ther. Pat.*, 11:1245–52.
Masuda, M., Nakashima, H., Ueda, T. et al. 1992. *Biochem. Biophys. Res. Commun.*, 189:845–50.
Miyata, T., Tokunaga, F., Yoneya, T. et al. 1989. *J. Biochem.*, 106:663–8.
Mori, T., Doi, R., Koizumi, M. et al. 2004. *Mol. Cancer Ther.*, 3:29–37.
Müller, A., Homey, B., Soto, H. et al. 2001. *Nature*, 410:50–6.
Murakami, T., Maki, W., Cardones, A.R. et al. 2002. *Cancer Res.*, 62:7328–34.
Murakami, T., Nakajima, T., Koyanagi, Y. et al. 1997. *J. Exp. Med.*, 186:1389–93.
Murakami, T., Zhang, T-Y., Koyanagi, Y. et al. 1999. *J. Virol.*, 73:7489–96.
Nagasawa, T., Kikutani, H. and Kishimoto, T. 1994. *Proc. Natl. Acad. Sci. U.S.A.*, 91:2305–9.
Nakamura, T., Furunaka, H., Miyata, T. et al. 1988. *J. Biol. Chem.*, 263:16709–13.
Nakashima, H., Masuda, M., Murakami, T. et al. 1992. *Antimicrob Agents Chemother.*, 36:1249–55.
Nanki, T., Hayashida, K., El-Gabalawy, H.S. et al. 2000. *J. Immunol.*, 165:6590–8.
Oberlin, E., Amara, A., Bachelerie, F. et al. 1996. *Nature*, 382:833–5.
Ojida, A., Mito-oka, Y., Sada, K. et al. 2004. *J. Am. Chem. Soc.*, 126:2454–63.
Piovan, E., Tosello, V., Indraccolo, S. et al. 2005. *Blood*, 105:931–9.
Robledo, M.M., Bartolome, R.A., Longo, N. et al. 2001. *J. Biol. Chem.*, 276:45098–105.
Rubin, J.B., Kung, A.L., Klein, R.S. et al. 2003. *Proc. Natl. Acad. Sci. U.S.A.*, 100:13513–8.
Sanz-Rodriguez, F., Hidalgo, A. and Teixido, J. 2001. *Blood*, 97:346–351.
Schols, D., Struyf, S., Van Damme, J. et al. 1997. *J. Exp. Med.*, 186:1383–8.
Schrader, A.J., Lechner, O., Templin, M. et al. 2002. *Br. J. Cancer*, 86:1250–6.
Scotton, C.J., Wilson, J.L., Milliken, D. et al. 2001. *Cancer Res.*, 61:4961–5.
Scotton, C.J., Wilson, J.L., Scott, K. et al. 2002. *Cancer Res.*, 62:5930–8.
Scozzafava, A., Mastrolorenzo, A. and Supuran, C.T. 2002. *J. Enz. Inhib. Med. Chem.*, 17:69–76.
Seibert, C. and Sakmar, T.P. 2004. *Curr. Pharm. Design.*, 10:2041–62.
Spoo, A.C., Lübbert, M., Wierda, W.G. et al. 2007. *Blood*, 109:786–91.
Taichman, R.S., Cooper, C., Keller, E.T. et al. 2002. *Cancer Res.*, 62:1832–7.
Takenaga, M., Tamamura, H., Hiramatsu, K. et al. 2004. *Biochem. Biophys. Res. Commun.*, 320:226–32.
Tamamura, H., Esaka, A., Ogawa, T. et al. 2005. *Org. Biomol. Chem.*, 3:4392–4.
Tamamura, H. and Fujii, N. 2005. *Expert Opin. Ther. Targets*, 9:1267–82.
Tamamura, H., Fujisawa, M., Hiramatsu, K. et al. 2004. *FEBS Lett*, 569:99–104.
Tamamura, H., Hiramatsu, K., Kusano, S. et al. 2003. *Org. Biomol. Chem.*, 1:3656–62.
Tamamura, H., Hiramatsu, K., Mizumoto, M. et al. 2003. *Org. Biomol. Chem.*, 1:3663–9.
Tamamura, H., Hori, A., Kanzaki, N. et al. 2003. *FEBS Lett*, 550:79–83.
Tamamura, H., Ojida, A., Ogawa, T. et al. 2006. *J. Med. Chem.*, 49:3412–5.
Tamamura, H., Omagari, A., Hiramatsu, K. et al. 2001. *Bioorg. Med. Chem. Lett.*, 11:1897–902.
Tamamura, H., Omagari, A., Oishi, S. et al. 2000. *Bioorg. Med. Chem. Lett.*, 10:2633–7.
Tamamura, H., Sugioka, M., Odagaki, Y. et al. 2001. *Bioorg. Med. Chem. Lett.*, 11:359–362 and 2409.
Tamamura, H. and Tsutsumi, H. 2006. *Chem. Biol.*, 13:8–10.
Tamamura, H., Tsutsumi, H., Masuno, H. et al. 2006. *Org. Biomol. Chem.*, 4:2354–7.
Tamamura, H., Xu, Y., Hattori, T. et al. 1998. *Biochem. Biophys. Res. Commun.*, 253:877–82.
Tashiro, K., Tada, H., Heilker, R. et al. 1993. *Science*, 261:600–3.
Tsukada, N., Burger, J.A., Zvaifler, N.J. et al. 2002. *Blood*, 99:1030–7.
Vermeire, K., Hatse, S., Princen, K. et al. 2004. *Antiviral Res.*, 62:A42–A43.
Xu, Y., Tamamura, H., Arakaki, R. et al. 1999. *AIDS Res. Hum. Retroviruses*, 15:419–27.
Zannettino, ACW., Farrugia, A.N., Kortesidis, A. et al. 2005. *Cancer Res.*, 65:1700–9.

ANTIMICROBIAL AGENTS AND CHEMOTHERAPY, June 2008, p. 2111–2119 Vol. 52, No. 6
0066-4804/08/$08.00+0 doi:10.1128/AAC.01299-07

Potent Synergistic Anti-Human Immunodeficiency Virus (HIV) Effects Using Combinations of the CCR5 Inhibitor Aplaviroc with Other Anti-HIV Drugs▽

Hirotomo Nakata,[1,2] Seth M. Steinberg,[3] Yasuhiro Koh,[2] Kenji Maeda,[1] Yoshikazu Takaoka,[4] Hirokazu Tamamura,[5] Nobutaka Fujii,[5] and Hiroaki Mitsuya[1,2]*

Experimental Retrovirology Section, HIV and AIDS Malignancy Branch, Center for Cancer Research, National Cancer Institute, National Institutes of Health, Bethesda, Maryland 20892[1]; Kumamoto University Graduate School of Medical and Pharmaceutical Sciences, Departments of Infectious Diseases and Hematology, Kumamoto 860-8556, Japan[2]; Biostatistics and Data Management Section, Center for Cancer Research, National Cancer Institute, National Institutes of Health, Bethesda, Maryland 20892[3]; Ono Pharmaceutical Co. Ltd., Osaka 618-8585, Japan[4]; and Graduate School of Pharmaceutical Sciences, Kyoto University, Sakyo-ku, Kyoto 606-8501, Japan[5]

Received 8 October 2007/Returned for modification 19 November 2007/Accepted 21 March 2008

Aplaviroc (AVC), an experimental CCR5 inhibitor, potently blocks in vitro the infection of R5-tropic human immunodeficiency virus type 1 (R5-HIV-1) at subnanomolar 50% inhibitory concentrations. Although maraviroc is presently clinically available, further studies are required to determine the role of CCR5 inhibitors in combinations with other drugs. Here we determined anti-HIV-1 activity using combinations of AVC with various anti-HIV-1 agents, including four U.S. Food and Drug Administration-approved drugs, two CCR5 inhibitors (TAK779 and SCH-C) and two CXCR4 inhibitors (AMD3100 and TE14011). Combination effects were defined as synergistic or antagonistic when the activity of drug A combined with B was statistically greater or less, respectively, than the additive effects of drugs A and A combined and drugs B and B combined by using the Combo method, described in this paper, which provides (i) a flexible choice of interaction models and (ii) the use of nonparametric statistical methods. Synergistic effects against R5-HIV-1_{Ba-L} and a 50:50 mixture of R5-HIV-1_{Ba-L} and X4-HIV-$1_{ERS104pre}$ (HIV-$1_{Ba-L/104pre}$) were seen when AVC was combined with zidovudine, nevirapine, indinavir, or enfuvirtide. Mild synergism and additivity were observed when AVC was combined with TAK779 and SCH-C, respectively. We also observed more potent synergism against HIV-$1_{Ba-L/104pre}$ when AVC was combined with AMD3100 or TE14011. The data demonstrate a tendency toward greater synergism with AVC plus either of the two CXCR4 inhibitors compared to the synergism obtained with combinations of AVC and other drugs, suggesting that the development of effective CXCR4 inhibitors may be important for increasing the efficacies of CCR5 inhibitors.

CCR5 is a member of the G-protein-coupled, seven-transmembrane-segment receptors, which comprise the largest superfamily of proteins in the body (30). In 1996, it was revealed that CCR5 serves as one of the two essential coreceptors for the entry of human immunodeficiency virus type 1 (HIV-1) into human $CD4^+$ cells, thereby serving as an attractive target for possible interventions against HIV-1 infection (1, 9, 40, 42). Consequently, scores of small-molecule CCR5 inhibitors which exert potent activity against R5-tropic HIV-1 (R5-HIV-1) were identified (2, 10, 19, 35). Aplaviroc (AVC), a spirodiketopiperazine derivative, represents one such experimental small-molecule CCR5 inhibitor (17, 18). AVC binds to human CCR5 with a high affinity, blocks HIV-1 gp120 binding to CCR5, and exerts potent activity against a wide spectrum of laboratory and primary R5-HIV-1 isolates, including multidrug-resistant HIV-1 isolates (50% inhibitory concentrations, 0.2 to 0.6 nM) (17, 18). Maraviroc (MVC) is another small-molecule CCR5 inhibitor which has become the first CCR5 inhibitor approved for the treatment of AIDS and HIV-1 infection by the U.S. Food and Drug Administration (FDA). One possible concern over the long-term use of CCR5 inhibitors is the change of viral tropism, which enables the virus to use the CXCR4 receptor (20, 41); therefore, CCR5 inhibitors are unlikely to be used as single agents. Assessments of the interaction of CCR5 inhibitors with other anti-HIV-1 agents should thus help provide an understanding of the role of CCR5 inhibitors and help design regimens to be used for the treatment of individuals infected with HIV-1.

In the present study, we determined the effects against R5-HIV-1_{Ba-L} of AVC in combination with various anti-HIV-1 agents which affect other steps of the viral life cycle, including a nucleoside reverse transcriptase inhibitor, zidovudine (ZDV); a nonnucleoside reverse transcriptase inhibitor, nevirapine (NVP); a protease inhibitor, indinavir (IDV); and a fusion inhibitor, enfuvirtide (ENF). We assessed the synergistic effects of AVC in combination with CXCR4 inhibitors as well as the other drugs described above against a mixture of R5-HIV-1_{Ba-L} and X4-HIV-$1_{ERS104pre}$ (designated HIV-$1_{Ba-L/104pre}$). In the present study, we also developed an evaluation system, designated the Combo method, which provides (i) a flexible choice of interaction models, (ii) the use of nonparametric statistical methods to obtain *P* values for comparison, and (iii) flexibility with respect to experimental design (e.g., checkerboard and constant-ratio designs). The present data suggest that AVC exerts antiviral synergy when it is

* Corresponding author. Mailing address: Departments of Infectious Diseases and Hematology, Kumamoto University School of Medicine, 1-1-1 Honjo, Kumamoto 860-8556, Japan. Phone: (81) 96-373-5156. Fax: (81) 96-363-5265. E-mail: hm21q@nih.gov.

▽ Published ahead of print on 31 March 2008.

used with other classes of anti-HIV-1 agents but apparently not when it is used with other CCR5 inhibitors. The present data also demonstrate a tendency toward greater synergism with AVC plus either of the two CXCR4 inhibitors examined in comparison to the synergism obtained with combinations of AVC and other FDA-approved drugs, suggesting that the development of effective CXCR4 inhibitors may be important for increasing the efficacies of CCR5 inhibitors.

MATERIALS AND METHODS

Antiviral agents. AVC is an experimental CCR5 inhibitor containing a spirodiketopiperazine core, as described previously (18, 19, 26). TAK779, SCH-C, and AMD3100 were synthesized as described previously (2, 7, 35). ZDV was purchased from Sigma (St. Louis, MO). IDV was kindly provided by Japan Energy Inc. (Tokyo, Japan). TE14011 and ENF were synthesized as described previously (36, 37). NVP was a kind gift from Boehringer Ingelheim Pharmaceuticals Inc. (Ridgefield, CT).

Viruses. R5-HIV-$1_{Ba\text{-}L}$ was obtained from the AIDS Research and Reference Reagent Program (13). X4-HIV-$1_{ERS104pre}$ was isolated from a drug-naïve patient with AIDS (33). These HIV-1 isolates were propagated in phytohemagglutinin-stimulated peripheral blood mononuclear cells (PHA-PBMCs), and the culture supernatants were harvested and stored at −80°C until use (22). In certain experiments, a 50:50 mixture of HIV-$1_{Ba\text{-}L}$ and HIV-$1_{ERS104pre}$ (HIV-$1_{Ba\text{-}L/104pre}$) was prepared.

Assay for in vitro anti-HIV-1 activity. PBMCs were isolated from the buffy coats of HIV-1-seronegative individuals by Ficoll-Hypaque density gradient centrifugation and were cultured at a concentration of 10^6 cells/ml in RPMI 1640-based culture medium supplemented with 10% fetal calf serum (FCS; HyClone Laboratories, Logan, UT), penicillin (50 U/ml), and streptomycin (50 μg/ml) (10% FCS–RPMI) with 10 μg/ml PHA for 3 days prior to the anti-HIV-1 activity assay in vitro. PHA-PBMCs (10^6/ml) from a 3-day culture were resuspended in 10% FCS–RPMI containing 10 ng/ml interleukin-2 and plated into each well of 96-well microculture plates (10^5 per well). Each of the test compounds was added as a single agent or in combination with another agent to each well of the microculture plates. For assessment of the effects of a combination of any two drugs, three threefold serial concentrations were chosen on the basis of the dose-response curve at which the percent inhibition values increased linearly.

The cells were subsequently exposed to 50 50% tissue culture infectious doses ($TCID_{50}$s) of HIV-$1_{Ba\text{-}L}$ or a mixture of 25 $TCID_{50}$s of HIV-$1_{Ba\text{-}L}$ and 25 $TCID_{50}$s of HIV-$1_{ERS104pre}$ and incubated at 37°C in humidified air containing 5% CO_2. On day 7 of culture, the cell-free culture supernatants were harvested and the HIV-1 p24 antigen levels in the supernatants were determined with a fully automated chemiluminescent enzyme immunoassay system (Lumipulse F; Fujirebio Inc., Tokyo, Japan) (18, 23). All the assays were performed in duplicate, and each experiment was conducted on 5 to 10 different occasions. No cytotoxicity was observed at the highest concentrations of each agent, as assessed by the trypan blue dye exclusion method.

Mathematical analysis: the Combo method. We assessed the effects of drug combinations using the combination index (CI), calculated with CalcuSyn software (BioSoft, Cambridge, United Kingdom), which was based on the median-effect method developed by Chou and Talalay (3, 4). For experiments with combinations of the same drug, serially diluted drug concentrations were chosen on the basis of the 50% effective concentrations (EC_{50}s), and each drug was combined with itself at the same concentration. As in the original method, CIs of <1, 1, and >1 were judged to represent synergism, additivity, and antagonism, respectively.

It should be noted that the Chou and Talalay median-effect method (3, 4) alone does not allow us to statistically compare the effects of the combinations. Thus, we devised a new method for evaluation of the effects of drug combinations, designated the Combo method. For the Combo method used in the present study, we used three concentrations of one drug (drug A) and three concentrations of the other drug (drug B) and combined the drugs at three different concentrations, preparing nine (3 × 3) combination cultures, and we obtained nine determinations of HIV-1 p24 concentrations (each combination assay was performed in duplicate). More precisely, three combinations were examined: the same drug A combination (drug A and drug A), the same drug B combination (drug B and drug B), and the combination of drug A and drug B. A full view of the data obtained with the drug combinations can be visualized (as shown in the Results section) in three-dimensional (3-D) figures by the use of Microsoft Excel software (version 11.0, 2004; Microsoft Corporation, Redmond, WA), based on the method of Prichard and colleagues (27, 28, 29). It is of note that with the Bliss independence method, the predicted additive effects at each combination point are subtracted from the inhibitory effects of the combination determined from the experimental drug combination assay, generating percent synergy values, and the points plotted above the predicted additive effects represent synergism, while the points below the plane represent antagonism. Using the Bliss independence method, we calculated percent synergy values for the nine determinations described above, and the average value was further computed, generating a mean percent synergy value (%$synergy^{mean}$). We repeated this assay for each drug combination 5 or 10 times on different occasions. These 5 or 10 %$synergy^{mean}$ values thus obtained for a set of combinations (drug A-drug A, drug B-drug B, and drug A-drug B) were compared with the other data sets (5 or 10 %$synergy^{mean}$ values) by the Wilcoxon rank sum test, generating P values for each combination set. All P values are two-tailed and have not been formally adjusted for multiple comparisons. However, in the context of the several experiments and comparisons performed, P values of <0.01 would clearly indicate statistical significance, while differences with values of $0.01 < P < 0.05$ would indicate strong trends.

TABLE 1. Anti-HIV-1 activity of each drug in the assay system

Virus	Compound	EC (nM) for anti-HIV-1 activity[a]			
		50%	75%	90%	95%
Ba-L	AVC	0.7 ± 0.4	4.0 ± 4.0	16 ± 15	25 ± 14
	SCH-C	6.8 ± 6.0	31 ± 18	94 ± 43	131 ± 64
	TAK779	20 ± 14	127 ± 83	332 ± 192	576 ± 224
	ZDV	18 ± 4.0	58 ± 3.0	128 ± 54	178 ± 49
	NVP	19 ± 2.0	36 ± 11	127 ± 39	149 ± 47
	IDV	29 ± 7.0	44 ± 12	75 ± 18	87 ± 13
	ENF	11 ± 4.0	46 ± 5.0	82 ± 14	98 ± 16
104pre	AMD3100	26 ± 8.0	96 ± 21	193 ± 51	257 ± 46
	TE14011	4.0 ± 1.0	16 ± 7.0	50 ± 11	78 ± 17

[a] The EC_{50}, EC_{75}, EC_{90}, and EC_{95} values were determined by using PHA-PBMCs isolated from three different donors and the inhibition of p24 Gag protein production as the end point. All assays were conducted in triplicate. The results shown represent the arithmetic means (±1 standard deviation) of the values from three independently conducted assays.

RESULTS

Activities of anti-HIV-1 agents in PHA-PBMCs. We first determined the antiviral potencies of seven anti-HIV-1 agents (AVC, SCH-C, TAK779, ZDV, NVP, IDV, and ENF) against HIV-$1_{Ba\text{-}L}$ employing PHA-PBMCs as target cells (Table 1). AVC had a potent inhibitory effect against HIV-$1_{Ba\text{-}L}$, with mean EC_{50}, EC_{75}, EC_{90}, and EC_{95} values of 0.7, 4, 16, and 25 nM, respectively. SCH-C and TAK779, which are both CCR5 inhibitors, also showed potent antiviral activity (but with less potent antiviral activity compared to that of AVC), with EC_{50}s of 6 and 20 nM, respectively. To determine the additive effects of AVC-AVC and AMD3100-AMD3100, we employed R5-HIV-$1_{Ba\text{-}L}$ and X4-HIV-$1_{ERS104pre}$ as the virus inocula, respectively, since AVC is inert against X4-HIV-1 and AMD3100 is inert against R5-HIV-1. These two agents were found to be potent against the virus, with EC_{50}s of 26 and 4 nM, respectively. No toxicity of any of the anti-HIV-1 agents was observed at concentrations up to 1.0 μM, as determined by examination of PHA-PBMCs (data not shown).

Same-drug combination and additivity. To determine whether combinations of two different anti-HIV-1 agents produced synergistic, additive, or antagonistic effects, we first attempted to establish an algorithm so that the effects of the combination of the same drug (i.e., drug A-drug A) represent

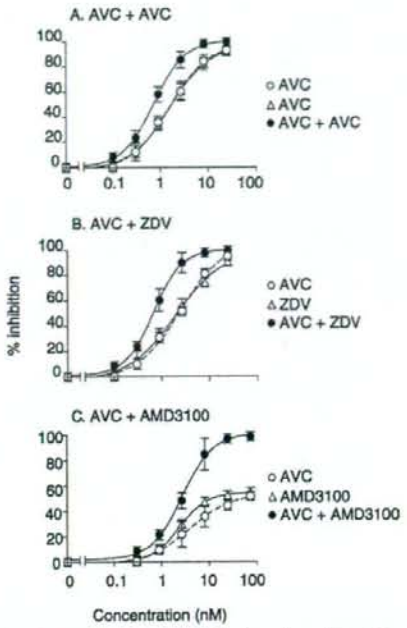

FIG. 1. Dose-response curves of single and combined drug assays. Three representative dose-response curves are shown. (A) Dose-response curve with the same-drug combination (AVC-AVC). PHA-PBMCs were exposed to R5-HIV-1_{Ba-L} and cultured in the presence of AVC alone or AVC-AVC over 7 days. AVC was serially diluted threefold to give concentrations in the range of 0.1 to 24.3 nM. The percent inhibition values were determined on the basis of the amounts of p24 Gag proteins in the culture supernatants. (B) AVC was combined with ZDV at a fixed ratio (1:11), and the assay was conducted as described above for panel A. (C) AVC (concentration range, 0.3 to 72.9 nM) was combined with AMD3100 at a 1:11 ratio. PHA-PBMCs were exposed to a 50:50 mixture of R5-HIV_{Ba-L} and X4-HIV-$1_{ERS104pre}$ and cultured in the presence of AVC alone, AMD3100 alone, or AVC-AMD3100. All assays were performed on 5 to 10 different occasions, and all the values shown represent the arithmetic means ± 1 standard deviation.

additivity. We determined the effects of combinations of the same drug for each of the seven anti-HIV-1 agents using the CIs dictated by the median-effect method (4). Figure 1A shows three representative dose-response curves of the percent inhibition of HIV-1 replication in the presence of a CCR5 inhibitor (AVC) alone, a reverse transcriptase inhibitor (ZDV) alone, a CXCR4 inhibitor (AMD3100) alone, or AVC plus AVC, ZDV, or AMD3100. A range of concentrations at which the percent inhibition values linearly increased was identified (Fig. 1A and B) and was used to examine the effects of any combination of two drugs chosen.

We found that the same-drug combination of AVC-AVC which gave a 50% reduction of HIV-1 replication produced a CI of 1.03 ± 0.09 (Table 2), indicating that this combination produced additivity on the basis of the median-effect method. However, that same-drug combination which gave 75, 90, and 95% reductions in viral replication produced CIs of 0.82, 0.71, and 0.68, respectively, which indicated that this same-drug combination produced synergistic effects. Synergistic effects were similarly indicated when the other anti-HIV-1 agents were examined as same-drug combinations in our analysis (Table 2).

The indication of synergism in the same-drug combination described above was thought to be a limitation or error inherent to the median-effect method or to stem from the variability of the biological data obtained. Since the median-effect method does not provide room for statistical analysis or a full view of the combination data, we examined the same data set using Microsoft Excel software, based on the method of Prichard and colleagues (27, 28, 29), which gives a graphical 3-D view of the entire data set. In the analysis of the AVC-AVC combination data, this method with Microsoft Excel software indicated that the combination of the highest AVC concentration (2.7 nM AVC and 2.7 nM AVC) that produced synergism gave a percent synergy value of 2.2, although other combinations were determined to be additive or antagonistic, giving an average (± standard deviation) percent synergy value of −1.8 ± 2.4 (Fig. 2A). The same-drug combinations of ZDV, NVP, and ENF similarly gave partial synergism (Fig. 2B, C, and E). However, the same-drug combination of IDV indicated synergism with all data points, with an average percent synergy value of 3.6 ± 2.2 (Fig. 2D). We predicted that the partial synergism seen with AVC, ZDV, NVP, and ENF and the entire synergism seen with IDV also represented a limitation or error inherent to the method of Prichard and colleagues (27, 28, 29) or the variability of the biological data obtained.

AVC acts in synergy with ZDV, NVP, IDV, and ENF to block the replication of HIV-1_{Ba-L} in PHA-PBMCs. Considering that one of the main reasons for the partial synergism described above could stem from the variability of the cell-based assay data used in the present work, we used standard nonparametric statistical analysis methods to evaluate the differences. To this end, we conducted the drug-combination assay in duplicate and determined the $\%synergy^{mean}$ values in three settings: (i) drug A-drug A, (ii) drug B-drug B, and (iii) drug A-drug B. Experiments testing the drug A-drug A combination and the drug B-drug B combination were conducted on 10 different occasions, while the drug A-drug B combinations assay was conducted on 5 different occasions. As shown in Fig. 3A, as

TABLE 2. CIs against HIV-1 obtained with mixtures of the same compounds at various inhibitory concentrations

Virus	Combination[b]	CI[a]			
		50%	75%	90%	95%
Ba-L	AVC + AVC	1.03 ± 0.09	0.82 ± 0.10	0.71 ± 0.10	0.68 ± 0.09
	ZDV + ZDV	1.08 ± 0.14	0.95 ± 0.18	0.84 ± 0.23	0.81 ± 0.22
	NVP + NVP	0.99 ± 0.09	0.81 ± 0.11	0.69 ± 0.12	0.66 ± 0.14
	IDV + IDV	1.02 ± 0.06	0.91 ± 0.05	0.79 ± 0.07	0.76 ± 0.06
	ENF + ENF	1.04 ± 0.08	0.89 ± 0.08	0.75 ± 0.09	0.73 ± 0.11
104pre	AMD + AMD	1.12 ± 0.12	0.88 ± 0.09	0.69 ± 0.09	0.67 ± 0.10
	TE + TE	1.05 ± 0.15	0.90 ± 0.11	0.80 ± 0.13	0.78 ± 0.13

[a] Drug interactions of same-drug combinations were analyzed by using CIs. CIs were calculated on the basis of the model of Chou and Talalay (3, 4) with CalcuSyn software (BioSoft). Originally, CIs of <1, 1, or >1 indicated a synergistic effect, an additive effect, and antagonism, respectively. The drugs were combined at a 1:1 ratio, and all assays were conducted in duplicate. The results shown represent the arithmetic means (±1 standard deviation) of the CIs at various inhibitory concentrations (50%, 75%, 90%, and 95%) from 10 independently conducted assays.

[b] AMD, AMD3100; TE, TE14011.

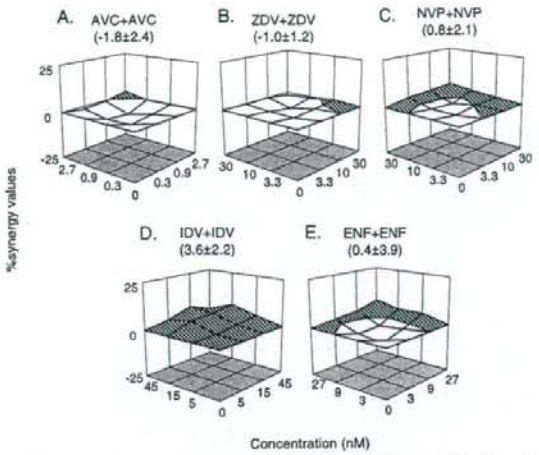

FIG. 2. Effects of same-drug combinations. The serially diluted anti-HIV-1 agents AVC (A), ZDV (B), NVP (C), IDV (D), and ENF (E) were combined with the same agent diluted under the same conditions; PHA-PBMCs were exposed to R5-HIV-1_{Ba-L} and cultured in the presence of the drugs combined. The combination effects (percent synergy values on the vertical z axis) were determined on the basis of the Bliss independence method. In the 3-D graphs, obtained on the basis of the method of Prichard et al. (27, 28, 29), the average percent synergy values at each concentration derived from 10 experiments were plotted. The hatched area represents synergism (percent synergy values, >0), while the open area represents additivity or antagonism (percent synergy values, ≤0). Numbers in parentheses represent the average percent synergy values (±1 standard deviation). The x and y axes indicate the concentrations of the drug tested (nM). All assays were performed in duplicate, and each experiment was independently conducted 10 times.

expected, the same-drug combination assays with AVC and ZDV produced relatively low average %synergy^{mean} values of −1.8 and −1.0, respectively. However, the AVC-ZDV combination gave a high average %synergy^{mean} value of 8.0. When we examined the difference among the AVC-AVC, ZDV-ZDV, and AVC-ZDV data using the Wilcoxon rank sum test, there was a statistically significant difference between the AVC-AVC and the AVC-ZDV data (P = 0.002) as well as between the ZDV-ZDV and the AVC-ZDV data (P = 0.003). The same was true when we examined the effects of NVP, IDV, and ENF in combination with AVC (Fig. 3B to D). With these data, we determined that if both the drug A-drug A and drug B-drug B combinations gave relatively low %synergy^{mean} values and a significant difference between the drug A-drug B combination and the same-drug combinations was detected, we would judge that there was significant synergism. When we plotted the average percent synergy value for the combination of drugs A and B at each different concentration on a point-by-point basis by the method of Prichard and colleagues (27, 28, 29), the results showed substantially higher levels of synergism for all data points (Fig. 3E to H). The average percent synergy values for AVC-ZDV, AVC-NVP, AVC-IDV, and AVC-ENF were 8.0 ± 3.1, 5.2 ± 2.3, 6.4 ± 1.9, and 7.2 ± 1.2, respectively, which corroborated the interpretation of the data shown in Fig. 3A to D. Thus, we interpreted that the addition

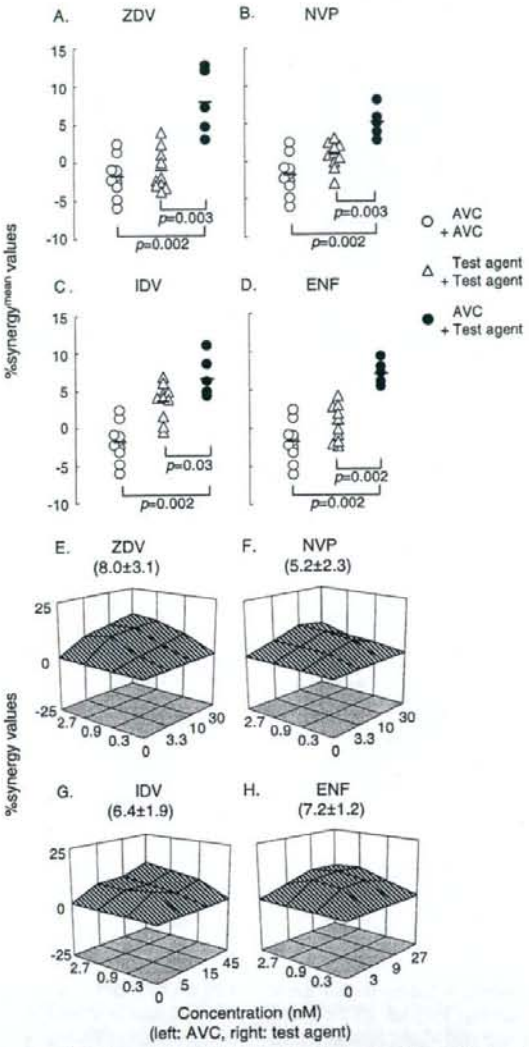

FIG. 3. Effects of AVC in combination with other anti-HIV-1 agents against R5-HIV-1_{Ba-L}. Drug combination assays were conducted, and the %synergy^{mean} values (the mean of the nine percent synergy values from each set of the data) are shown in three settings: (i) AVC-AVC, (ii) test agent (to be combined with AVC)-test agent, and (iii) AVC-test agent (A to D). The AVC-AVC combination and the test agent-test agent combination were tested on 10 different occasions, while the AVC-test agent combination assay was done on 5 different occasions. The differences in the %synergy^{mean} values between the three settings were analyzed by using the Wilcoxon rank sum test. The short bars indicate the arithmetic means. The combination effects are also shown in 3-D graphs, as determined on the basis of the method of Prichard et al. (see the legend to Fig. 2).

of AVC to each of the other agents produced significant synergism.

Effects of AVC in combination with SCH-C or TAK779 against R5-HIV-1_{Ba-L}. We next asked whether AVC in combi-

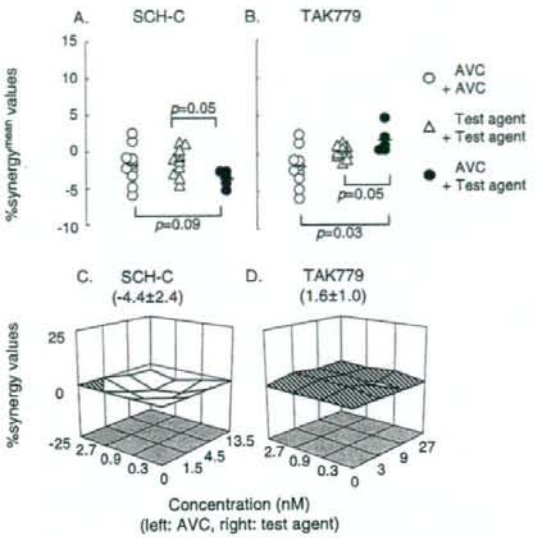

FIG. 4. Effects of AVC in combination with other CCR5 inhibitors. The effects of AVC in combination with SCH-C (A) or TAK779 (B) when they were exposed to R5-HIV-1_{Ba-L} are shown. No significant synergism was seen when AVC was combined with SCH-C or TAK779 compared with that seen with AVC-AVC. There was a trend toward antagonism when AVC–SCH-C with SCH-C–SCH-C and a trend toward synergism when AVC-TAK779 was compared with TAK779-TAK779. When these data were examined by the method of Prichard et al. (27, 29), AVC–SCH-C showed a mixed pattern but with an inclination toward antagonism (C), while AVC-TAK779 showed a mixed pattern but with an inclination toward synergy (D).

nation with SCH-C or TAK779 had synergistic activity against HIV-1_{Ba-L} (Fig. 4). The difference between the AVC-AVC and the AVC–SCH-C combinations was not statistically significant ($P = 0.09$), while there was evidence of a trend toward antagonism between the SCH-C–SCH-C and the AVC–SCH-C combinations ($P = 0.05$). It was interesting that when these data were examined by the method of Prichard and colleagues (27, 28, 29), a mixed pattern with an inclination toward antagonism was seen, with an average percent synergy of -4.4 ± 2.4. We also examined whether AVC had significant combination effects when it was combined with TAK779. There was a trend toward a statistically significant difference between AVC-AVC and AVC-TAK779 ($P = 0.03$) as well as TAK779-TAK779 and AVC-TAK779 ($P = 0.05$). However, when these data were plotted in the chart by the method of Prichard and colleagues (27, 28, 29), the pattern was a mixed one, with a low average percent synergy (1.6 ± 1.0), suggesting that synergism would be at a low level. However, it was noted that the same set of data for the combination of AVC and SCH-C produced CI values of 1.05 (at a 50% inhibitory effect) and 0.58 (at a 90% inhibitory effect), indicating that there was synergism between AVC and SCH-C, as analyzed on the basis of the median-effect method of Chou and Talalay (3, 4). It was thought that there was a propensity toward an overestimation of the combination effects toward synergism when the median-effect method was used.

Combination effects of AVC in a mixture of R5-HIV-1_{Ba-L} and X4-HIV-$1_{ERS104pre}$. AVC exerts no antiviral activity against X4-HIV-1 (18, 23), although the HIV-1 population seen in individuals with HIV-1 infection often comprises both R5- and X4-HIV-1 populations. Hence, it would be reasonable to use a CCR5 inhibitor plus a CXCR4 inhibitor to treat individuals with HIV-1 infection (6). Thus, we attempted to examine effects of the combination of AVC and either AMD3100 and TE14011 against HIV-$1_{Ba-L/104pre}$.

It is thought that the replication kinetics of HIV-1 strains tend to affect the results of any antiviral assay, in particular, when more than one HIV-1 isolate is employed in one assay. We therefore first conducted a set of experiments in order to delineate the replication curves for both the R5-tropic (HIV-1_{Ba-L}) and X4-tropic (HIV-$1_{ERS104pre}$) strains used in this study. It was confirmed that the two strains had comparable replication kinetics and that the p24 values of both strains were comparable over 7 days when the amount of each strain inoculated was adjusted on the basis of the $TCID_{50}$ for the strain (data not shown). Moreover, the amounts of HIV-1 p24 produced by PBMCs that were exposed to the mixture of the R5- and X4-tropic strains and cultured in the presence of a high concentration of AVC were comparable to the amounts of HIV-1 p24 from PBMCs that were similarly treated but that were cultured in the presence of a high concentration of AMD3100 (Fig. 1C). These data suggested that HIV-1_{Ba-L} and HIV-$1_{ERS104pre}$ replicate comparably in cell cultures inoculated with the 50:50 mixture of the viruses. To determine the additive effects of AVC-AVC and AMD3100-AMD3100, we employed R5-HIV-1_{Ba-L} and X4-HIV-$1_{ERS104pre}$ as the target viruses, respectively, since AVC is inert against X4-HIV-1 and AMD3100 is inert against R5-HIV-1.

The AVC-AMD3100 combinations produced %synergy^{mean} values significantly different from those for AVC-AVC ($P = 0.002$) and those for AMD3100-AMD3100 ($P = 0.005$) (Fig. 5A). When these combination data were examined in the 3-D model of Prichard and colleagues (27, 28, 29), apparently high levels of synergism were seen for all data points, with an average percent synergy value of 8.0 ± 4.4 (Fig. 5G). When TE14011 was combined with AVC, synergism was similarly seen, with an average percent synergy value of 8.2 ± 4.5 (Fig. 5H). The %synergy^{mean} values for AVC-ENF were also greater than those for AVC-AVC ($P = 0.005$) and less than those for ENF-ENF ($P = 0.04$); however, when the level of synergism was examined in the 3-D model, it appeared to be relatively lower, with an average percent synergy value of 4.8 ± 4.2 (Fig. 5I).

We next examined the effect of AVC in combination with one of the three FDA-approved anti-HIV-1 agents, ZDV, NVP, and IDV. The %synergy^{mean} values obtained with AVC-ZDV or AVC-NVP were greater than those obtained with AVC-AVC, ZDV-ZDV, and NVP-NVP (P values for all comparisons, ≤ 0.005; Fig. 5D and E). In the 3-D model, synergism was also observed for ZDV and NVP in combination with AVC (Fig. 5J and K). AVC-IDV produced no significant difference in the %synergy^{mean} values compared to those for IDV-IDV ($P = 0.2$), although the effect of AVC-IDV was significantly different from the effect of AVC-AVC (Fig. 5F), and a substantial level of percent synergy was also seen in the 3-D model (Fig. 5L).